Title
The KSHV protein ORF68 is a proteasome-manipulating protein required for DNA packaging

Author
Gardner, Matthew Ryan

Publication Date
2018

Peer reviewed|Thesis/dissertation

The KSHV protein ORF68 is a proteasome-manipulating protein required for DNA packaging

By

Matthew Ryan Gardner

A dissertation submitted in partial satisfaction of the

requirements for the degree of

Doctor of Philosophy

in

Infectious Diseases and Immunity

in the

Graduate Division

of the

University of California, Berkeley

Committee in charge:

Professor Britt A. Glaunsinger, Chair
Professor Laurent Coscoy
Professor Andreas Martin

Summer 2018

Abstract

The KSHV protein ORF68 is a proteasome-manipulating protein required for DNA packaging

by

Matthew Ryan Gardner

Doctor of Philosophy in Infectious Diseases and Immunity

University of California, Berkeley

Professor Britt A. Glaunsinger, Chair

Herpesviruses are large, double-stranded DNA viruses that have evolved over millions of years to become master manipulators of cellular machinery. Herpesviral research has taught us a great deal not only about strategies of viral replication and pathogenesis, but also about how cellular pathways work in the absence of infection. The end goal of viral infection is the production of progeny virions, which involves the packaging viral genomes into nascent capsids. This process is mechanistically conserved across the three herpesvirus subfamilies, with at least seven viral proteins being required for successful packaging to occur. Of these proteins, six have well characterized functions during the packaging process, while the function of the seventh remains largely unknown. In Kaposi's sarcoma-associated herpesvirus (KSHV), this protein is encoded by ORF68 and here we aimed to elucidate its role in DNA packaging.

We first generated an ORF68 mutant of KSHV that contained a premature termination codon (ORF68^{PTC}) and confirmed that ORF68 was not required for viral gene expression or DNA replication but was essential for infectious virion production. Additionally, the KSHV ORF68^{PTC} virus did not cleave or package viral DNA and exclusively accumulated immature B-capsids. Further biochemical characterization of ORF68 revealed several novel activities for this protein that significantly expand our understanding of its function. Unexpectedly, we found that ORF68 robustly binds DNA and exhibits metal-dependent nuclease activity towards dsDNA *in vitro*. These observations suggest a role in binding and catalytically processing the viral genome during packaging.

Additionally, protein-protein interaction profiling of ORF68 revealed an association with multiple subunits of the proteasome, the main protein degradation apparatus of the cell. This led us to hypothesize that KSHV might control protein abundance, in part, through the ORF68-proteasome interaction. In support of this hypothesis, we revealed that ORF68 contains a canonical gate-opening motif observed in proteasome-interacting proteins. Deletion or blocking of this motif in ORF68 inhibited the degradation of a model substrate in transfected cells, suggesting that ORF68 may assemble on proteasomes to control substrate access. Notably, deletion of this motif from

ORF68 in the context of KSHV infection prevented progeny virion production, indicating that this function is central to its role in the viral replication cycle. Finally, we observed proteasomes concentrated within replication compartments together with ORF68. Collectively, these data lead to a model in which ORF68 interactions with the proteasome may control protein turnover to facilitate viral DNA packaging.

Dedication

To my wife and best friend, Katherine,
my parents, Nora and Dennis,
and my siblings Dennis and Bria.

Without your love, support, guidance,
and patience this work would not have
been possible. I am unreasonably lucky
to have you all in my life.

Table of Contents

List of Figures / Tables

Acknowledgements

Britt – Thank you for the opportunity to start this new area of research in your lab, even when I meandered about and got into the weeds of protein purification. You are truly a one-of-a-kind mentor and your constant support and encouragement has made me into the scientist that I am today. Your guidance and instruction on how to give an interesting talk has forever changed not only the way in which I present my research, but also the way in which I think about science. I can't imagine my scientific career without you and I will be forever grateful.

Angelica and Allison – Although Angelica has shouldered the burden of sitting adjacent to me for much longer, Allison has had a crash course in the rambling, if occasionally useful, discourse of the protein bay. A trial by fire that not many new lab members could stomach, you both have had a profound impact on not only my work, but who I am as a person today. I truly do not know how I would have done the majority of the work that I have without both of your brilliant suggestions, thoughtful insight, and constant sanity-checks.

Zoe – It's almost hard to remember my first days in the Glaunsinger Lab, with you as my mentor, yet I still find myself starting so many sentences with, "Well, Zoe always said…". You not only convinced me to join the lab in the first place, but set up my project in a way that only you could have done. Both the mentorship and friendship that you so freely give has shaped not only my life, but the Glaunsinger Lab for the foreseeable future.

The Glaunsinger Lab – What is there to say to a group of individuals who I feel like I have truly grown up around? Not in the normal sense, but in the scientific and personal sense. You all made coming into the lab for 50+ hours a week not only bearable, but truly enjoyable. Your input and ideas are priceless and I am confident that you all will go on to do amazing things.

Martin Lab – Thank you to all of you who welcomed me to your Group Meetings and entertained my naïve questions about all of biochemistry (and in particular isoleucine bond angles). Although extensive, our weekly meetings made me a better critical thinker and opened my eyes to the wide world of the proteasome and biochemistry.

IDI Students – I'm sure some of you know how strongly I feel about our program, but I am extremely grateful to have met all of you and learned how to be a scientist alongside you. From my classmates in those first two years, to everyone who invited me to their practice qual, thank you for going on this journey with me.

Apurva – Saying that I know how far you'll go is kind of cheating because of how far you have already gone, but it was a privilege to teach you what I could about molecular biology. I very much look forward to how you will change the world in ways only you can.

To everyone who helped me along the way, but I did not have room to list: Thank you. You are forever in my thoughts and none of this would have been possible without you all.

Matthew Ryan Gardner

Curriculum Vitae

EDUCATION:

University of California Berkeley School of Public Health — August 2012 – August 2018
PhD, Department of Infectious Diseases and Immunity

The George Washington University CCAS — August 2007 – May 2011
B.S., Biology

RESEARCH EXPERIENCE:

Glaunsinger Lab – UC Berkeley — May 2013 – present
Graduate Student Researcher: Investigate the modulation of proteasome activity by KSHV through *in vitro* analysis of purified KSHV proteins.

Chiorini Lab – National Institutes of Health, NIDCR — May 2011 – August 2012
Molecular Biology and Therapeutics Branch
Intramural Research Fellow: *In vivo* investigation of the ties between Hepatitis Delta Virus and Sjögren's Syndrome using Recombinant Adeno-Associated Virus.

Hawdon Lab – The George Washington University — May 2008 – May 2011
Research Assistant: Analysis of the *Ancylostoma caninum* insulin-dependent transcription actor HLH-13.

PUBLICATIONS:

Gardner, M.R., and Glaunsinger, B.A. (2018). Kaposi's sarcoma-associated herpesvirus ORF68 is a DNA binding protein required for viral genome cleavage and packaging. J. Virol. JVI.00840–18–38.

Weller ML, Gardner MR, Bogus ZC, et al. "Hepatitis Delta Virus Detected in Salivary Glands of Sjögren's Syndrome Patients and Recapitulates a Sjögren's Syndrome-Like Phenotype *in Vivo*." *Pathogens & immunity*. 2016;1(1):12-40.

PRESENTATIONS:

2018 International Conference on EBV & KSHV, Madison, Wisconsin — July 2018
Oral: "The KSHV protein ORF68 is a proteasome-manipulating nuclease required for DNA packaging"

8th Annual Bay Area Virology Symposium, Berkeley, CA — June 2018
Oral: "The KSHV protein ORF68 is a proteasome-manipulating nuclease required for DNA packaging"

10th Annual CEND Symposium, Berkeley, CA — January 2018
Poster: "Manipulation of the Proteasome by Kaposi's Sarcoma-associated Herpesvirus"

HHMI Science Meeting, Bethesda, MD November 2017
Poster: “Manipulation of the Proteasome by Kaposi’s Sarcoma-associated Herpesvirus”

UC Berkeley Plant and Microbial Biology Retreat, Berkeley, CA September 2017
Oral: “Manipulation of the Proteasome by a KSHV-Encoded Protein Complex”

7th Annual Bay Area Virology Symposium May 2017
Poster: “Manipulation of the Proteasome by a KSHV-Encoded Protein Complex”

UC Berkeley MCB - BBS Retreat, Asilomar, CA January 2017
Oral: “Manipulation of the Proteasome by a KSHV-Encoded Protein Complex”

19th International Workshop on KSHV and Related Agents, Los Angeles, CA July 2016
Poster: “Inhibition of the Proteasome by the KSHV Protein ORF68”

8th Annual CEND Symposium, Berkeley, CA March 2016
Poster: “Inhibition of the Proteasome by the KSHV Protein ORF68”

UC Berkeley MCB - BBS Retreat Retreat, Asilomar, CA January 2016
Poster: “Inhibition of the Proteasome by the KSHV Protein ORF68”

Infectious Diseases and Immunity Seminar, Berkeley, CA September 2015
Oral: “Manipulation of the Ubiquitin-Proteasome System by KSHV”

40th Annual International Herpesvirus Workshop, Boise, ID July 2015
Poster: “Manipulation of the Ubiquitin-Proteasome System by Kaposi’s Sarcoma-associated Herpesvirus”

16th Annual Microbiology Student Group Symposium, Berkeley, CA April 2015
Oral: “Manipulation of the Ubiquitin-Proteasome System by Kaposi’s Sarcoma-associated Herpesvirus”

7th Annual CEND Symposium, Berkeley, CA January 2015
Poster: “Manipulation of the Ubiquitin-Proteasome System by KSHV”

GWU Student Research Competition, Washington, DC April 2011
Poster: “Sequencing and Homology of the Insulin-Dependent Transcription Factor HLH-13 of the Hookworm *Ancylostoma caninum*”

The Helminthological Society Research Competition, Washington, DC October 2010
Oral: “Sequencing and Homology of the Insulin-Dependent Transcription Factor HLH-13 of the Hookworm *Ancylostoma caninum*”

HONORS, AWARDS, AND FELLOWSHIPS:

Beattie Memorial Award for Excellence in Research	2018
Infectious Diseases and Immunity Leadership Award	2015
Berkeley Graduate Division Power Award	2012
NIH Post-Baccalaureate Intramural Research Training Award	2011 – 2012
National Society of Collegiate Scholars	2008
Scholars of Quantitative and Natural Sciences	2007 – 2011
GWU Board of Trustees Scholarship	2007 – 2011
GWU Alumni Award	2007 – 2011

TEACHING EXPERIENCE:

UC Berkeley – Molecular and Cellular Biology Department

Graduate Student Instructor

Immunology Laboratory (MCB 150), Instructor: Robert Beatty, PhD Spring 2015
Immunity and Disease (MCB 50), Instructor: Robert Beatty, PhD Spring 2014

UC Berkeley – Glaunsinger Lab

Graduate Student Mentor

Melody Lin: Undergraduate Student Researcher October 2017 – May 2018

Apurva Govande: Undergraduate Student Researcher January 2014 – May 2016
Currently, NSF Graduate Research Fellow Kranzusch Lab – Harvard University

Chapter 1: Introduction

Herpesviridae

Herpesviruses are ubiquitous pathogens that infect a wide range of species, from humans to coral (Vega Thurber et al., 2008). These large, enveloped, double-stranded DNA viruses establish life-long infectious through the process of viral latency. During latency, few viral genes are expressed and infected cells remain largely undetected by the host immune system. However, the viral genome stably persists in these cells and will periodically reactivate to enter the lytic replication cycle, producing new virions and potentially infecting new cells and hosts (Grinde, 2013). Nine herpesviruses are known to infected humans and almost all adult humans are infected with at least one of these viruses (Renner and Szpara, 2017). Human herpesviruses are generally classified into one of three subfamilies: alpha-, beta-, or gammaherpesviruses, each of which contain medically important pathogens (Davison et al., 2008). The alphaherpesviruses that commonly cause disease are herpes simplex (HSV) type 1 and type 2, the etiologic agents of oral and genital herpes, respectively, and varicella-zoster virus (VZV), which causes chickenpox and shingles (Azab and Osterrieder, 2017a). Human cytomegalovirus (HCMV) is the only medically-relevant member of the betaherpesvirus family and is the leading cause of congenital neurological disease (Beltran and Cristea, 2014). Additionally, HCMV is a major concern in solid tissue transplantation, where it can cause a variety of complications ranging from retinitis and hepatitis to transplant rejection and death (Goodrum, 2016). Important gammaherpesviruses include Epstein-Barr virus (EBV) and Kaposi's sarcoma-associated herpesvirus (KSHV). EBV is the cause of most infectious mononucleosis, while KSHV is the etiologic agent of Kaposi's sarcoma. Furthermore, both viruses can cause lymphoproliferative disorders, particularly in immunocompromised individuals (Ganem, 2006; Straus et al., 1993).

While the herpesvirus families vary widely in their tissue tropism, clinical manifestations, and genome size, they all follow the same overall gene expression cascade and replication cycle. Gene expression in herpesviruses is divided between the lytic and latent replication cycles. During latency, no progeny virions are produced and only a small subset of genes are expressed, together with viral microRNAs, which primarily regulate cell growth and maintain the viral episome (Piedade and Azevedo-Pereira, 2016; Ueda, 2018). During the lytic cycle, all viral genes are expressed, the viral genome is replicated, and new virions are produced. The lytic cycle is additionally characterized by the temporal cascade in which the genes are expressed. Lytic genes are generally broken down into three kinetic classes, immediate early, delayed early, and late genes. Immediate early genes are the first to be expressed and are not reliant on the expression of other viral genes. These genes produce proteins that both evade the immune response and prime the cell for the expression of delayed early genes. Delayed early genes are responsible for the replication of the viral genome and encode the machinery required for the expression of late genes (Gruffat et al., 2016). Here, alphaherpesviruses differ from beta and gammaherpesviruses, which encode a conserved set of proteins that are responsible for the transcription of late genes (Davis et al., 2015a). Late genes themselves are primarily capsid components and proteins required for the egress of mature virions. The expression kinetics of late genes are notable in that they require the replication of the viral genome for expression. Inhibition of the viral polymerase

prevents late gene expression, while immediate early and early genes are unaffected (Li et al., 2018).

Kaposi's sarcoma-associated herpesvirus (KSHV)

Kaposi's sarcoma-associated herpesvirus is the eighth herpesvirus found to infect humans. Although the medical community had been aware of Kaposi's sarcoma for many years, it was a disease largely associated with elderly Mediterranean men. With the rise of HIV and AIDS, Kaposi's sarcoma became much more rampant, becoming the major AIDS-defining illness of the 1980's (Ganem, 2006). Today, it remains the leading cause of cancer in sub-Saharan Africa, as the etiologic agent of not only Kaposi's sarcoma, but also plasmablastic multicentric Castleman's Disease and primary effusion lymphoma. Additionally, KSHV can cause complications during solid-tissue organ transplantation, as well as KS-immune reconstitution syndrome and KSHV-inflammatory cytokine syndrome (Dittmer and Damania, 2016).

KSHV is a *Rhadinovirus* and a member of the gammaherpesvirus subfamily, which also contains EBV. The dsDNA KSHV genome is about 170 kb, which encodes for approximately 90 proteins and several microRNAs. Many of these proteins have not been studied and their functions are often inferred from other herpesviruses (Davis et al., 2015b). KSHV appears to default to the latent cycle of infection, particularly in cultured cells. In KSHV, latency is maintained by the protein LANA, which also tethers the viral DNA, present as a circular episome, to host chromatin. Lytic replication is initiated by the protein "replication and transcription activator" (RTA) encoded by ORF50, which binds to a number of promoters present in the viral genome (Ueda, 2018). The balance between latency and lytic reactivation is not well understood during infection, but it is thought that in a KS lesion, only 1 – 2 % of infected cells are in the lytic cycle at any given time (Ganem, 2006). Like EBV, KSHV can infect multiple cell types, including endothelial cells, monocytes, and dendritic cells, but its primary reservoir appears to be B-cells (Dittmer and Damania, 2016).

While only recently discovered, KSHV, like all herpesviruses, is truly ancient. As long as there have been humans, they have been infected with herpesviruses. Over the course of millions of years, KSHV has evolved to become a consummate manipulator of its mammalian host. This makes it not only a very successful virus, but also a unique tool for scientists. By studying how KSHV controls and subverts host cell biology, we can learn a great deal not only about strategies of viral pathogenesis and how they can be combated, but also about how the targeted pathways work in the absence of infection.

DNA packaging in herpesviruses

Herpesviruses produce large, complex virions that necessarily have an intricate assembly and maturation process. The production of progeny virions is both highly orchestrated and tightly controlled, requiring myriad proteins to perform their roles synchronously to produce mature, infectious virions. At their core, mature virions contain the double-stranded DNA genome, which is packaged into the icosahedral capsid under enormous pressure, at the limit of what is achievable in a non-crystalline state (McElwee et al., 2018). The capsid itself is made up of a number of proteins, which assemble into a T=16 icosahedron with a diameter of approximately 125 nm (Heming et al., 2017). The genome-containing capsid is further coated with the

proteinaceous tegument, which contains a variety of viral proteins and RNA, as well as small amounts of host cell-derived macromolecules (Abernathy et al., 2014). All of these layers are finally enclosed within the viral envelope, a lipid bilayer derived from the host cell that is studded with viral glycoproteins (Heming et al., 2017).

The process of virion production is of particular interest as it is the final stage in the viral replication cycle and its disruption can prevent the infection of new hosts. Furthermore, by perturbing only the final step in viral replication, one can produce DNA-free viral particles that could be used in a vaccination regimen (Pavlova et al., 2013). While the exact makeup of virions varies slightly between the herpesvirus families, each having unique envelope glycoproteins as dictated by their differing tropisms, the mechanisms by which virions are assembled remain well conserved (Azab and Osterrieder, 2017b). A particularly well conserved stage of virion assembly is the packaging of replicated viral genomes into newly formed capsids. This process is evolutionarily ancient, sharing many features with the DNA packaging of bacteriophages, which are viruses of an entirely different domain of life (Selvarajan Sigamani et al., 2013).

The process of DNA packaging begins with newly replicated viral genomes and immature procapsids. During viral DNA replication, the genome is replicated as head-to-tail concatemers, separated by an arbitrary number of terminal repeats (TR). In KSHV, the TRs are present in 20 – 40 copies made up of an 801 base-pair, highly repetitive subunit with a GC content of 85% (Habison et al., 2017). Procapsids are the first stage of capsid production, where the major and minor capsid proteins are assembled onto scaffolding proteins, which are subsequently proteolytically digested and removed from the capsid lumen during DNA packaging (Rixon et al., 1988). Once both concatemeric genomes and procapsids are present, a viral enzyme complex called the terminase binds to the genomes and brings them to the procapsid where it docks with the portal complex, present at only one vertex of the capsid (Heming et al., 2017). The terminase then threads the genome through the portal into the capsid in an ATP-dependent manner (Heming et al., 2014). Upon encountering the TRs, the terminase cleaves the genome, releasing the capsid that now contains one copy of the viral genome (Adelman et al., 2001). These DNA-containing capsids will go on to mature further by budding through the nuclear envelope, acquiring a golgi-derived double membrane and tegument proteins, and finally fusing with host cell membrane, being released as a mature virion (Smith, 2017). Mature virions have one lipid membrane studded with viral glycoproteins that surrounds the proteinaceous tegument, which is in turn surrounds the icosahedral capsid that contains one copy of the viral genome, maintained under extraordinary pressure (Mettenleiter, 2002).

DNA packaging requires seven viral proteins, without which there is no cleavage of the viral genome and subsequent maturation of virions. In KSHV, these proteins are: ORF43, the portal protein, ORF7, ORF29, and ORF67.5, which make up the terminase holoenzyme, ORF32 and ORF19, members of the vertex-specific complex, and ORF68, whose role remains largely mysterious (Heming et al., 2017). These proteins have mostly been studied in HSV-1, but given the importance of the DNA packaging process, the different herpesvirus families are unlikely to have diverged significantly. In HSV-1, the terminase is composed of UL28, UL33, and UL15, which have not been well studied together, but their independent activities have produced a plausible model of the DNA packaging reaction. UL28 (KSHV ORF7) first binds to the replicated viral genome and scans until it locates a specific DNA structure within the terminal repeat. This is

supported by the observation that UL28 will bind DNA probes that have been denatured and reannealed with much greater affinity than the original canonically base-paired probe (Adelman et al., 2001). Once the terminal repeats have been located, the terminase can then cleave at two specific sites within one of the terminal repeat subunits. This is most likely accomplished by UL15 (KSHV ORF29) which has been shown to have DNA nicking activity *in vitro* and contains an RNase H-like nuclease fold (Selvarajan Sigamani et al., 2013). UL15 additionally contains Walker A and B motifs, which are typical of ATPase enzymes and it is thought that this is what generates the energy needed to processively thread the genome into the capsid (Yu, 1998). These two proteins, along with UL33 (KSHV ORF67.5), come together to form the terminase holoenzyme. However, to efficiently dock with the capsid, two further proteins are required, UL17 (KSHV ORF32) and UL25 (KSHV ORF19), which are members of the vertex-specific complex. This complex is composed of many proteins and is associated with the vertices of the icosahedral capsid, but for DNA packaging, these two specific proteins aid in the docking of the terminase holoenzyme with the portal protein, which occupies only one vertex of the capsid (Newcomb et al., 2006; Thurlow et al., 2006). In contrast to the majority of these proteins, the portal protein has been studied in both KSHV (ORF43) and HSV-1 (UL6). There are several models of the structure that it forms, both by cryo-electron tomography (Cardone et al., 2007a), and by cryo-electron microscopy (McElwee et al., 2018). These structures show that the portal protein extends from outside of the capsid into the lumen, creating a channel through which DNA can be translocated. The final protein, UL32 (KSHV ORF68), has not been studied in depth, but there is a report of it acting as a disulfide isomerase. In this capacity, it alters the disulfide bonds of the viral protease, which then allows cleavage of the capsid scaffolding proteins (Albright et al., 2014). While not directly related to DNA packaging, the scaffolding protein must be removed from the lumen of the capsid, which is generally thought to occur during the packaging reaction itself (Heming et al., 2017). The DNA packaging process and required proteins are reviewed in Figure 1.1 and Table 1.1.

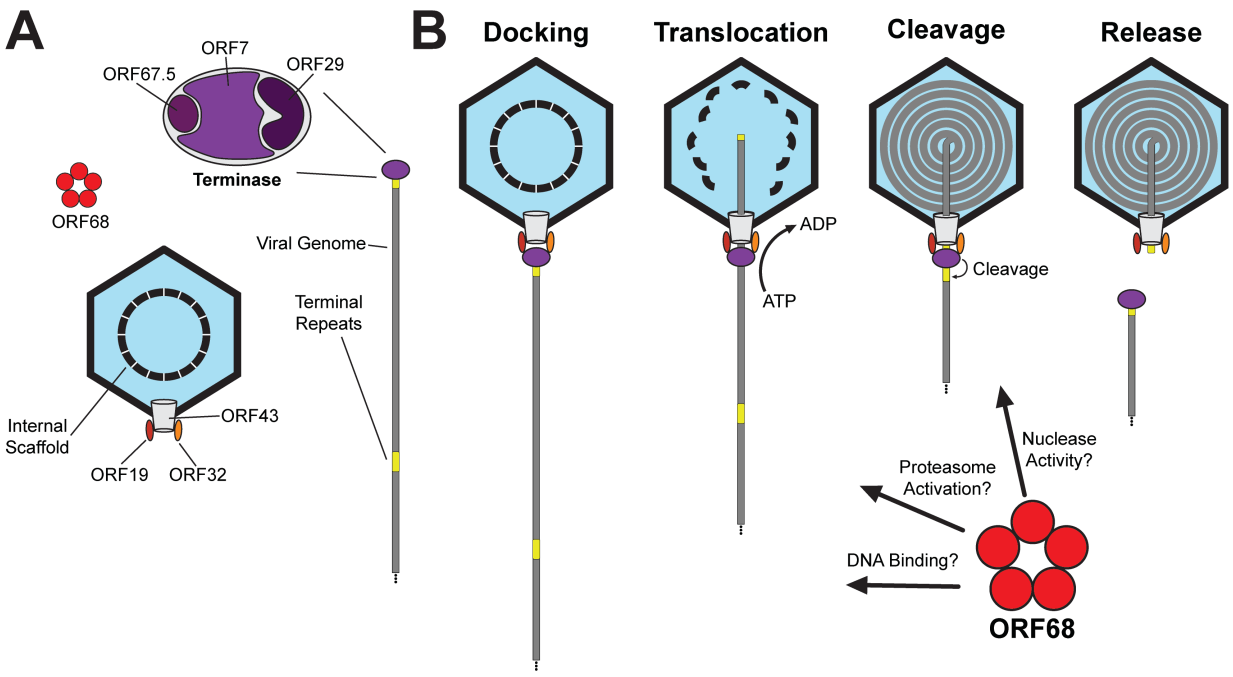

Figure 1.1: Model of DNA packaging in *Herpesviridae*. (A) Labeled representations of the required components of viral DNA packaging in KSHV. **(B)** The terminase holoenzyme (ORF7, ORF29, and ORF67.5) bind to the concatemeric viral genome at the terminal repeats, bringing it to immature capsids. The terminase interfaces with ORF19 and ORF32 to properly orient the genome for translocation through the portal complex (ORF43). The terminase processively translocates the genome into the capsid using ATP hydrolysis, displacing the scaffolding proteins. Once the capsid is full, the terminase encounters another set of terminal repeats and the genome is cleaved. The now full capsid is released and the terminase can go on to package additional capsids. ORF68 is the only protein required for this process without a defined function.

Table 1.1: Proteins required for viral DNA packaging

Alphaherpesvirus	Betaherpesvirus	Gammaherpesvirus		
HSV-1	**HCMV**	**EBV**	**KSHV**	**Function**
UL6	UL104	BBRF1	ORF43	Portal Protein
UL17	UL93	BGLF1	ORF32	Vertex-Specific-Complex: Docking
UL25	UL77	BVRF1	ORF19	Vertex-Specific-Complex: Docking
UL28	UL56	BALF3	ORF7	Terminase Subunit: DNA Binding
UL33	UL51	BFRF1A	ORF67.5	Terminase Subunit
UL15	UL89	BGRF1/BDRF1	ORF29	Terminase Subunit: Nicking, ATPase
UL32	UL52	BFLF1	ORF68	Unknown

The Proteasome

The proper regulation of protein homeostasis is a vital part of all known life. A great deal of thought and effort is put into understanding the production of proteins, but the removal of

proteins from the cell is equally important. Proteases are responsible for the degradation of proteins, cleaving the peptide bonds that hold them together and allowing for the recycling of amino acids into new proteins. However, both the production and destruction of proteins are energy-intensive processes and therefore must be tightly controlled (Yedidi et al., 2017). In eukaryotic cells, this is accomplished by the ubiquitin-proteasome system, where proteins are tagged for degradation by the covalent attachment of a small protein called ubiquitin. Ubiquitinated proteins are then trafficked to the proteasome where they are degraded in an ATP-dependent manner (Worden et al., 2017). The proteasome is a large (~2.5 MDa), ATP-dependent, chambered protease that is responsible for the majority of protein degradation in eukaryotic cells. Proteasomes can also be found in bacteria and archaea, although they do not rely on ubiquitin in these systems, revealing the truly ancient nature of these proteases (Budenholzer et al., 2017).

However, both the proteasome and ubiquitin have roles outside of the ubiquitin-proteasome system. Mono-ubiquitination, where a single ubiquitin molecule it attached instead of a chain, most often plays a role in cellular signaling, such as in histone regulation or endocytosis (Hicke, 2001). In general, the attachment of a ubiquitin chain consisting of four subunits is required for efficient proteasomal degradation, but there are several examples of ubiquitin-independent proteasomal degradation. These most often take the form of intrinsically disordered proteins, which are rapidly degraded by the proteasome. While they are not entirely understood, these proteins are often stabilized upon binding their interaction partners, shielding them from ubiquitin-independent degradation by the proteasome. This has been hypothesized to be a quality-control mechanism to ensure only bound complexes persist in the cell (Erales and Coffino, 2014).

In eukaryotic cells, the proteasome is a modular enzyme composed of several sub-complexes, each of which is in turn composed of individual subunits. All of the main proteolytic machinery is housed in the 20S core particle, which is made up of four heteroheptameric rings, stacked axially to create a barrel-shaped complex. There are two types of rings, called α- and β-, with the α-rings residing on the ends of the barrel and the β-rings residing in the center. The β-rings contain the six protease active sites, two for each type of proteolytic activity (Kish-Trier and Hill, 2013). These activities are; trypsin-like, cleaving after basic residues, chymotrypsin-like, cleaving after hydrophobic residues, and caspase-like, cleaving after acidic residues (Yedidi et al., 2017). The α-rings serve to close the barrel of the 20S, ensuring that proteins which have not been marked for degradation do not encounter the active sites. However, proteins that have been condemned to degradation need to be translocated into the lumen of the 20S core, and the α-rings form a “gate” structure for this purpose. Natively, this structure is closed, occluding access to the proteolytic chamber. Upon binding of certain other protein complexes there is a change in conformation or “opening” of the gate, which then allows access to the 20S lumen (Kish-Trier and Hill, 2013).

The α-rings additionally serve as interaction sites for the other sub-complexes of the proteasome. There are several different “proteasome activators” which can bind to the 20S core peptidase and facilitate the degradation of proteins. In mammalian cells, the 11S cap, PA200, and ECM29, have all been shown to have α-ring binding and gate-opening activity, but by far the best studied proteasome activator is the 19S regulatory particle (RP) (Pick and Berman, 2013). The

19S RP is itself composed of two sub-complexes, the Base and the Lid. The Base is a heterohexameric ring that binds to the 20S α-ring and has gate-opening activity. The Lid is a complex structure which sits to the side of the Base, but also reaches down to contact the outside of the 20S core. The Lid is responsible for recognizing and binding to ubiquitin chains on condemned proteins, removing the ubiquitin so that it may be recycled by the cell, and allowing the target protein to be engaged by the Base. This engagement occurs when a terminus or unstructured region of the target protein is threaded through the central pore of the Base. Once engaged, the Base uses the power provided by ATP hydrolysis to processively thread and unfold the substrate protein, translocating the now unfolded polypeptide chain into the lumen of the 20S core, where it is degraded. This is possible because the 19S RP, as well as other proteasome activators, contain gate-opening motifs that are responsible for their gate-opening (or "activating") activity. This is accomplished by the small, carboxyl-terminal motif of "Hb-Y-X" or Hydrophobic-Tyrosine-any amino acid, which sits in hydrophobic pockets on the 20S α-ring, causing the gate-opening conformational change. Deletion of any part of this motif, or extension beyond the motif, ablates the gate opening activity, preventing degradation of target proteins (Bard et al., 2018).

The extraordinary complexity of this system is emblematic of the central role it plays in many diverse cellular processes. The most obvious of these is the simple degradation of proteins that are no longer required by the cell, but even this is more nuanced than it seems. For instance, some of the degraded proteins are shuttled into the immune surveillance pathway and are presented on MHCI molecules. These peptides serve to alert the immune system to changes in the cellular environment, such as infection, and allow the compromised cells to be destroyed (Platteel et al., 2017). Outside of immune surveillance, proteasome-mediated protein degradation also serves as a quality control mechanism during translation. Up to 30% of newly-translated proteins are immediately degraded by the proteasome due to translation errors or misfolding at the ribosome (Wang et al., 2013). Additionally, the proteasome plays a role in cell signaling, as its activity is required to progress through the cell cycle. The proteasomal degradation of certain cell cycle-related proteins is what signals the cell to move on to the next phase, meaning that proteasome misfunction can lead to cell cycle arrest (Adams, 2004). The proteasome even participates in cellular processes without degrading proteins, such as the post-translational processing of proteins as is the case for NF-κB, or the initiation of transcription (Chen, 2005; Durairaj and Kaiser, 2014).

Being indispensable to many cellular processes, it is unsurprising that the ubiquitin-proteasome system is often manipulated by viruses. HIV tat has been shown to inhibit the binding of the 11S proteasome activator to the 20S core peptidase to inhibit the production of immunogenic peptides and evade detection by the immune system (Seeger et al., 1997). Similarly, the Hepatitis B protein X (HBx) has also been observed to interact with the 20S proteasome. The exact nature of this interaction remains to be defined, but overexpression of HBx inhibited the degradation of c-*Jun* and Arg-β-galactosidase, which are both known proteasome substrates. Furthermore, inhibition of proteasome activity with small molecule inhibitors negatively impacted viral replication *in vivo*, suggesting that proteasome function is required for the Hepatitis B viral replication cycle (Minor and Slagle, 2014). Proteasome inhibition has also been observed to inhibit viral replication and cause apoptosis in primary effusion

lymphoma cells, which are cells derived from a classic KSHV B-cell cancer (Saji et al., 2011). Similar to HIV tat and HBx, the KSHV protein LANA is known to directly interface with the 20S proteasome. In this context, the central repeat domain of the protein is very difficult for the proteasome to degrade, which causes the enzyme to stall once the protein is already engaged. Stalling of the proteasome in this manner prevents the further production of immunogenic peptides, helping KSHV to evade the immune response (Kwun et al., 2011).

Apart from LANA, KSHV encodes several proteins that interact with the ubiquitin-proteasome system. The majority of these target the ubiquitin side of the pathway to manipulate the cell cycle, apoptosis, cell signaling, and various immune responses. K3 and K5 are RING-CH-finger E3 ubiquitin ligases, proteins that can covalently attach ubiquitin to a target protein. These two particular proteins ubiquitinate both MHCI and γ-interferon receptor 1, promoting their endocytosis and degradation, in order to evade the host immune response (Ashizawa et al., 2012). KSHV ORF50 is primarily responsible for the induction of the lytic replication cycle, but also serves as a ubiquitin ligase that plays a role in the disruption of PML-nuclear bodies, which are an important part of the innate immune response (Izumiya et al., 2013). Finally, ORF64 displays deubiquitinase (DUB) activity, or the ability to remove ubiquitin chains that have been attached to proteins. DUBs are the counterpart to ubiquitin ligases and ORF64 removes ubiquitin chains from RIG-I to reduce interferon signaling (Ashizawa et al., 2012). These are the best examples of KSHV manipulating with the ubiquitin-proteasome system, but given the system's modularity and utility, there are likely many more.

Thesis Overview

This thesis aims to characterize the KSHV protein ORF68. Specifically, the role this protein plays in the process of viral DNA packaging and control of the host proteome through manipulation of the proteasome. Currently, KSHV ORF68 is entirely uncharacterized, with all activities and annotations inferred from homologous proteins in related herpesviruses.

This work represents the first description of ORF68, determining its kinetic class and expression profile, as well as the actual reading frame from which it is produced. Like homologous proteins in other herpesviruses, ORF68 is required for the cleavage of newly replicated genomes during packaging. However, unlike related proteins, we demonstrate the ability of ORF68 to robustly bind DNA and its association with metal-dependent nuclease activity. Furthermore, ORF68 was found to co-purify with the 20S proteasome both during transient transfection and viral infection. This putative interaction centered around the HbYX gate opening motif found in the carboxyl-terminus of ORF68. Deletion of this motif from ORF68 inhibited the degradation of a model substrate in cells and was absolutely required for infectious virion production.

The activities of ORF68 may at first seem disparate, but DNA is packaged into the virion under extremely high pressure, which precludes the presence of proteins associated with the genome inside of the capsid. Newly replicated viral genomes have numerous proteins associated with them, everything from the replication machinery itself to viral gene expression complexes. These proteins must necessarily be removed before the viral genome can be packaged and ORF68 may provide the mechanism through which this is accomplished. ORF68 can bind to the viral genome as well as the host proteasome, bringing the two together. The HbYX gate opening motif contained in ORF68 could activate the proteasome and degrade proteins associated with the

genome, allowing it to be efficiently packaged into nascent capsids. Furthermore, as with many viral proteins, ORF68 may have multiple roles during viral replication. ORF68 was observed to localize not only in the nucleus, where DNA replication and packaging occurs, but also in the cytoplasm. Here, ORF68 may act as a viral mimic of host proteasome activators, bypassing normal protein quality control machinery and allowing the virus to alter the host proteome.

Chapter 2: Kaposi's sarcoma-associated herpesvirus ORF68 is a DNA binding protein required for viral genome cleavage and packaging

Introduction

Following the expression of structural genes, capsids are assembled in the nucleus, first through the production of fragile procapsids (Rixon and McNab, 1999). Procapsids are formed by the binding and orientation of capsid proteins onto a protein scaffold, which is subsequently digested by the viral protease, allowing further maturation into A-, B-, or C-capsids. A-capsids lack both the protein scaffold and DNA genome and most likely arise from failed packaging events (Booy et al., 1991). B-capsids retain the cleaved protein scaffold and may represent a DNA-packaging failure, like A-capsids, or simply represent capsids that have not yet encountered the DNA-packaging machinery. Successful packaging of the viral genome, which displaces the digested scaffold proteins, results in the mature, DNA-containing C-capsids (Tandon et al., 2015).

The process of viral DNA replication generates head-to-tail concatemers, which are cleaved into unit-length genomes as they are packaged into immature capsids. In alpha and betaherpesviruses, DNA packaging is coordinated by seven viral proteins, each of which is essential for both cleavage and packaging of the newly replicated genomes (Heming et al., 2017). The proteins required for DNA packaging have been most extensively studied in the alphaherpesvirus Herpes Simplex virus type 1 (HSV-1), where the essential proteins are UL6, UL15, UL17, UL25, UL28, UL32, and UL33. UL6 forms a ring-shaped oligomer, which occupies one vertex of the icosahedral capsid, forming the portal through which the DNA is threaded during both packaging and unpackaging (Cardone et al., 2007b). UL28, UL15, and UL33 form the terminase motor, an ATP-dependent motor that physically threads the viral genome through the portal complex into the nascent capsid (Heming et al., 2014). Of the terminase motor, only UL28 has been shown to directly bind DNA (Adelman et al., 2001). However, UL15 and its homolog UL89 in betaherpesviruses have been shown to nick DNA substrates *in vitro* (Heming et al., 2017; Selvarajan Sigamani et al., 2013). UL17 and UL25 are part of the vertex-specific complex, which binds to the vertices of the assembled capsid, as well as to the portal complex, thereby aiding docking of the terminase motor (Newcomb et al., 2006; Thurlow et al., 2006). UL32 is the only protein that is required for DNA cleavage and packaging that lacks a well-defined function (Heming et al., 2017). However, UL32 contains a number of putative C-X-X-C type zinc finger domains and mutation of these conserved motifs results in altered di-sulfide patterns on the viral protease, which is involved in capsid assembly, supporting a role for UL32 in viral genome encapsidation (Albright et al., 2014).

Significantly less is known about the DNA packaging process in gammaherpesviruses such as Kaposi's sarcoma-associated herpesvirus (KSHV), although each of the packaging proteins described above are conserved. These include KSHV ORF7 (UL28; terminase subunit), ORF19 (UL25; vertex-specific complex), ORF29 (UL15; terminase subunit), ORF32 (UL17; vertex-specific complex), ORF43 (UL6; portal protein), ORF67.5 (UL33; terminase subunit), and ORF68 (UL32; unknown). Cryo-electron microscopy of KSHV capsids indicated that KSHV ORF43 forms the portal complex and that ORF32 is associated with vertices, consistent with studies in HSV-1 (Dai et al., 2014; Deng et al., 2008).

Given that role ORF68 and its homologs play during viral DNA packaging are largely unresolved across the herpesviridae, we sought to explore its function in more detail in KSHV-infected cells and *in vitro*. During lytic KSHV infection, many features of ORF68 were conserved with its alpha and betaherpesvirus homologs, such as localization to viral replication compartments, and its requirement for viral genome cleavage, packaging, and infectious virion production. Interestingly, biochemical analyses of recombinant ORF68 protein purified from mammalian cells revealed it to be a DNA-binding protein that is associated with dsDNA cleavage activity. These novel findings suggest that ORF68 plays a previously unappreciated role in KSHV genome processing and encapsidation.

Results

KSHV ORF68 is an early viral protein that localizes to viral replication compartments

Although KSHV ORF68 has not been characterized, its homologs in alpha and betaherpesviruses are expressed with late kinetics and are involved in viral DNA packaging (Albright et al., 2014; Borst et al., 2008). ORF68 shares 24.8% sequence identity with UL32, its best characterized homolog from HSV-1, including the five C-X-X-C motifs conserved across all the subfamily homologs (Albright et al., 2014). To characterize the expression kinetics and potential functions of KSHV ORF68, we generated a rabbit polyclonal antibody using recombinant ORF68 protein. We monitored the expression of ORF68 in KSHV-infected iSLK.BAC16 cells, a commonly used Caki-1 cell line containing a doxycycline (dox)-inducible version of the major viral lytic transactivator, ORF50 (RTA) (Brulois et al., 2012; Myoung and Ganem, 2011). Lytic reactivation of these cells upon dox treatment revealed that ORF68 expression begins as early as 6 hours post-reactivation and it is robustly expressed by 18 hours (Figure 1a). Its expression kinetics mimicked those of the KSHV delayed early protein ORF59, and it was not impacted by treatment with the viral DNA replication inhibitor phosphonoacetic acid (PAA), which blocks expression of viral late genes such as K8.1 (Figure 1a). Thus, KSHV ORF68 is a delayed early gene.

ORF68 has been alternatively annotated as a 467 amino acid (aa) protein and as a longer, 545 aa protein containing a 78 aa N-terminal extension (ORF68-Extended) (Figure 1c). However, on a western blot of iSLK.BAC16 lysate, ORF68 migrated as a single band at the predicted molecular weight (MW) of the 467 aa form (52kDa). To confirm that the 467 aa version was the expressed form in KSHV-infected cells, we cloned both versions into a mammalian expression vector and compared their migration pattern in transfected HEK293T cells to endogenous ORF68 in lytically-reactivated iSLK.BAC16 cells and the KSHV-infected B cell line TREx-BCBL1. Indeed, in both cell lines, only the 467 aa form of ORF68 was detected (Figure 1b).

We next evaluated the subcellular localization of ORF68 in reactivated iSLK.BAC16 and TREx-BCBL1 cells using immunofluorescence assays with the ORF68 antibody. To identify infected cells, cells were co-stained with an antibody against the viral polymerase processivity factor ORF59, which accumulates in viral replication compartments in the nucleus (Wu et al., 2001). We observed no ORF68 staining in unreactivated or ORF59-negative cells, but in reactivated cells ORF68 was present in both the cytoplasm and, more prominently, in the nucleus. In the cytoplasm, it was primarily diffuse, but also localized to some randomly distributed puncta and

larger aggregates close to the nucleus. In the nucleus, ORF68 was localized predominantly in viral replication compartments (Figure 2).

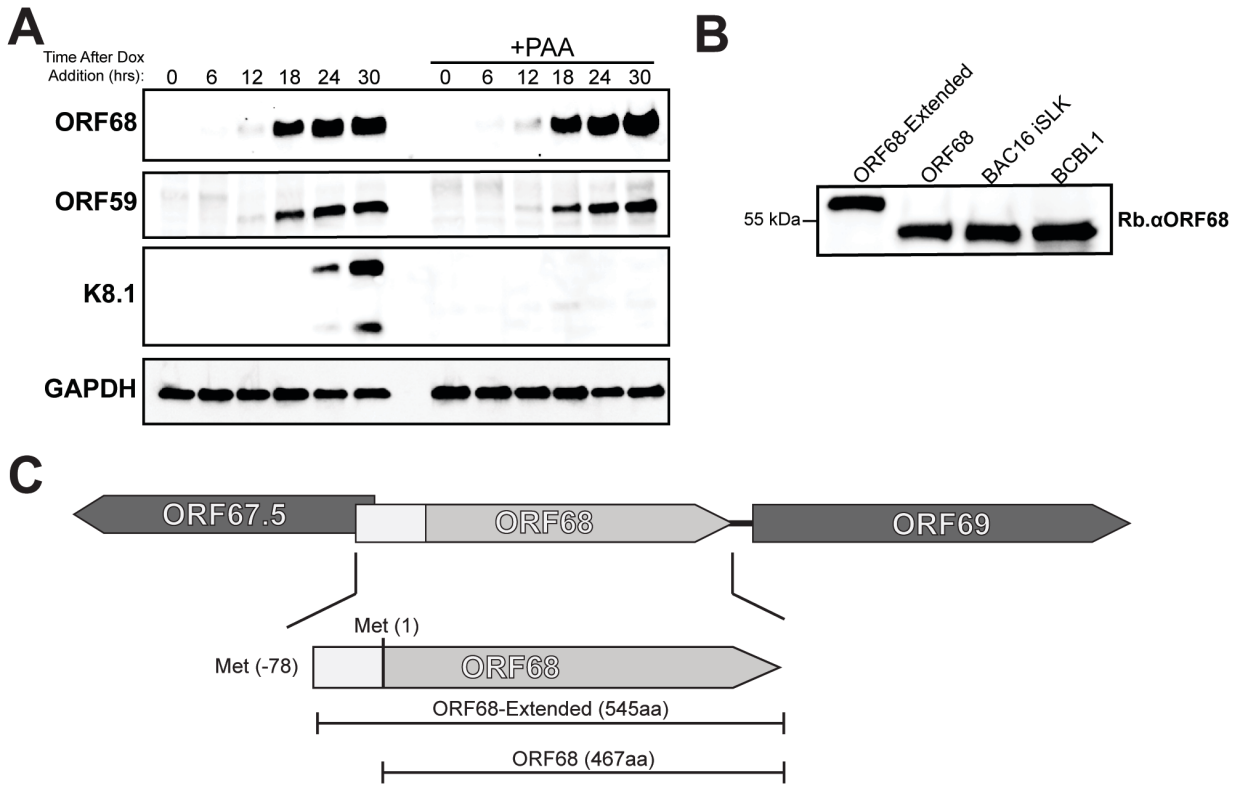

Figure 2.1. Characterization of the expression of KSHV ORF68. (A) Western blot showing the expression kinetics of ORF68 relative to the early protein ORF59 and the late protein K8.1 in iSLK.BAC16 cells post reactivation with doxycycline (dox). GAPDH serves as a loading control. **(B)** Anti-ORF68 western blot of lysates of HEK293T cells transfected with plasmids expressing either the extended (ORF68-Extended) or shorter form of ORF68, next to lysates of lytically reactivated iSLK.BAC16 and TREx-BCBL1 cells. Different amounts of lysate were loaded in each lane to account for differing ORF68-expression levels. **(C)** Diagram showing the genomic locus of ORF68, showing the two annotated forms, which differ by a 78 amino acid (aa) N-terminal extension.

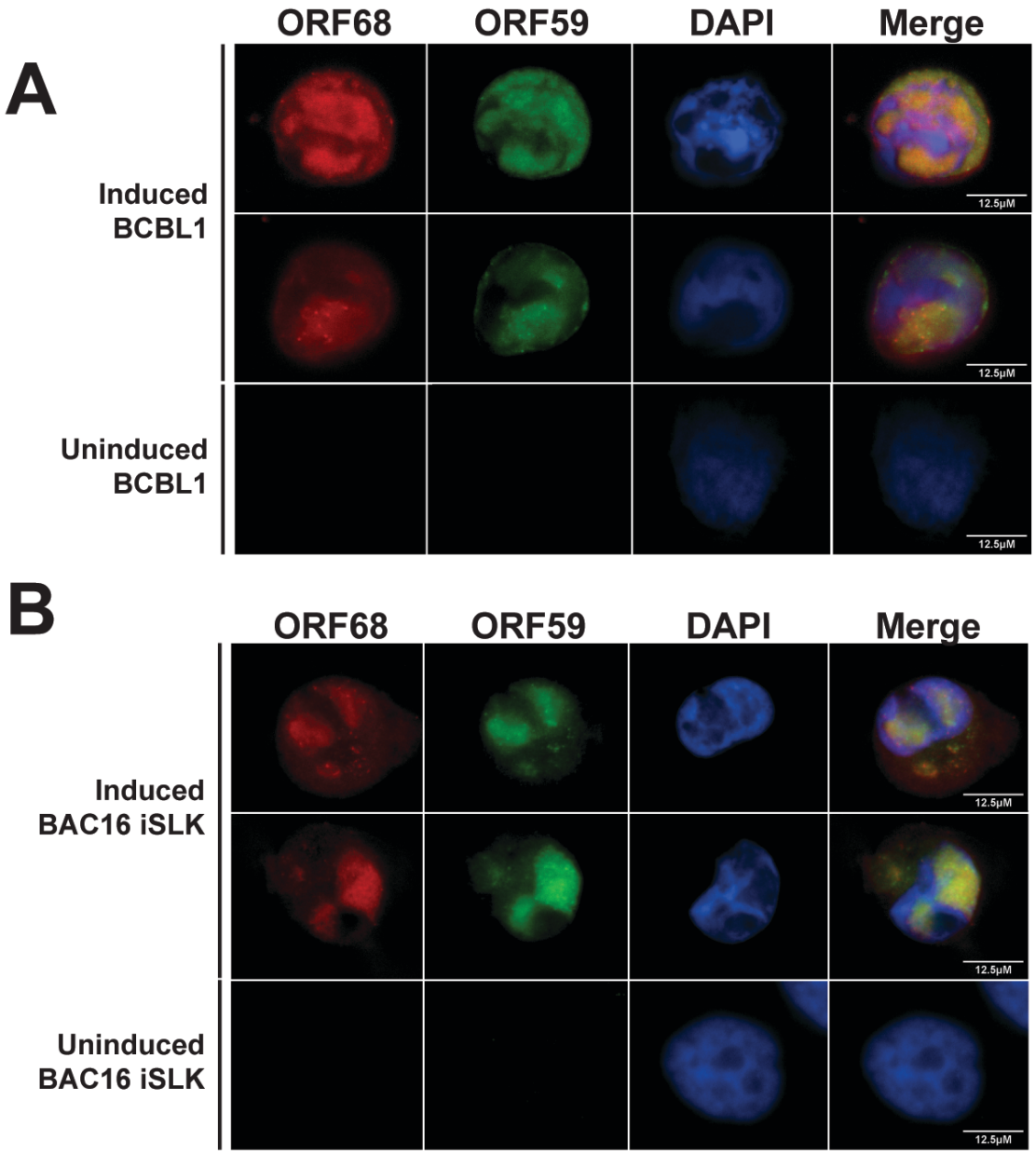

Figure 2.2. ORF68 localizes within replication compartments and in cytoplasmic puncta of KSHV infected cells. Reactivated and unreactivated TREx-BCBL1 **(A)** and BAC16.iSLK **(B)** cells were stained with antibodies to ORF68 (red), the viral replication compartment marker ORF59 (green), and DAPI (blue). The far-right panel shows the merged image.

KSHV lacking ORF68 maintains viral DNA replication and late gene expression, but does not produce infectious virions

To evaluate the role of ORF68 in the viral replication cycle, we generated an ORF68-deficient virus (ORF68^{PTC}) using the BAC16 Red Recombinase system (Brulois et al., 2012) by inserting two premature termination codons 15 nt downstream of the translation start site. This virus was used to establish a latently-infected cell line in iSLK cells. To ensure that any observed phenotypes were not due to secondary mutations, we also engineered the corresponding mutant rescue virus (ORF68^{PTC}-MR) (Figure 3a). Despite lacking ORF68 protein, the ORF68^{PTC} virus expressed both the delayed early protein ORF59 and the late protein K8.1 at levels similar to both the unmodified WT BAC16 KHSV and the ORF68^{PTC}-MR virus (Figure 3b). Furthermore, qPCR analyses of viral DNA revealed no significant difference in DNA replication between any of the viruses (Figure 3c). We then monitored production of infectious progeny virions using a supernatant transfer assay, in which the supernatant from reactivated infected iSLK cells is filtered and transferred to target cells. Because the BAC16-derived KSHV contains a virally-encoded, constitutively-expressed GFP reporter gene, infected recipient cells can be quantified by GFP expression using flow cytometry. Here, ORF68^{PTC} showed a marked defect, as no virus production was detectable, while both WT and ORF68^{PTC}-MR infected cells produced sufficient virus to infect nearly 100% of target cells (Figure 3d). Collectively, these data indicate that KSHV ORF68 is essential for a late stage event in the viral replication cycle.

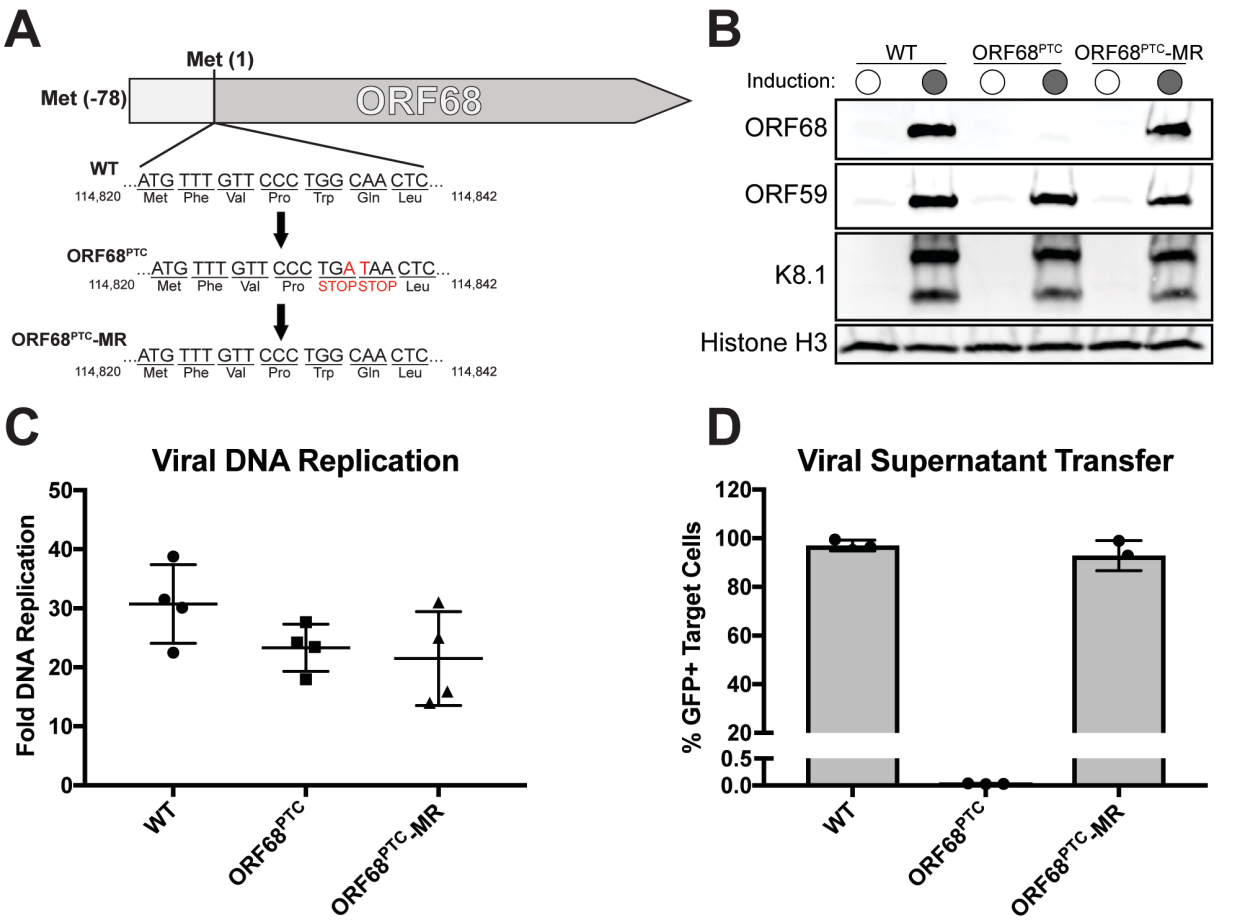

Figure 2.3. Characterization of the ORF68-deficient (ORF68^{PTC}) mutant virus. (A) Diagram depicting the genetic locus of ORF68 and the mutations inserted into the ORF68^{PTC} virus. **(B)** Western blots showing expression of the early ORF59 protein and the late K8.1 protein in WT, ORF68^{PTC}, and ORF68^{PTC}-MR viruses. Histone H3 served as a loading control. **(C)** DNA replication was measured by qPCR of the viral genome before and after induction of the lytic cycle. **(D)** Progeny virion production was assayed by supernatant transfer and flow cytometry of target cells.

In the absence of ORF68, KSHV DNA is not cleaved after replication

The above results, together with studies of alpha and betaherpesvirus ORF68 homologs (Albright et al., 2014; Borst et al., 2008), suggested a role for KSHV ORF68 in viral DNA encapsidation. We therefore established an assay similar to what has been used in other herpesviruses to measure packaging-associated KSHV DNA cleavage, which occurs within the 801 bp GC-rich terminal repeat (TR) sequences present in 20 – 40 tandem copies in the KSHV genome (Habison et al., 2017) (Figure 4a). Briefly, DNA was isolated from infected iSLK cells and the TR sequences were released by digesting the DNA with PstI-HF, which cleaves frequently within viral (and host) DNA, but not within the KSHV TRs. This should generate a ladder of TR sequences, representing the collection of individual cleavage events in the TRs that occur during packaging, which can be visualized by Southern blotting with a DIG-labeled TR probe. As expected, we observed a robust increase in the high MW uncleaved TRs following lytic reactivation of each sample, indicative of viral genome replication (Figure 4b). However, DNA from ORF68^{PTC} infected cells showed no evidence of TR cleavage, unlike DNA from WT and ORF68^{PTC}-MR infected cells, which displayed the expected laddering phenotype (Figure 4b).

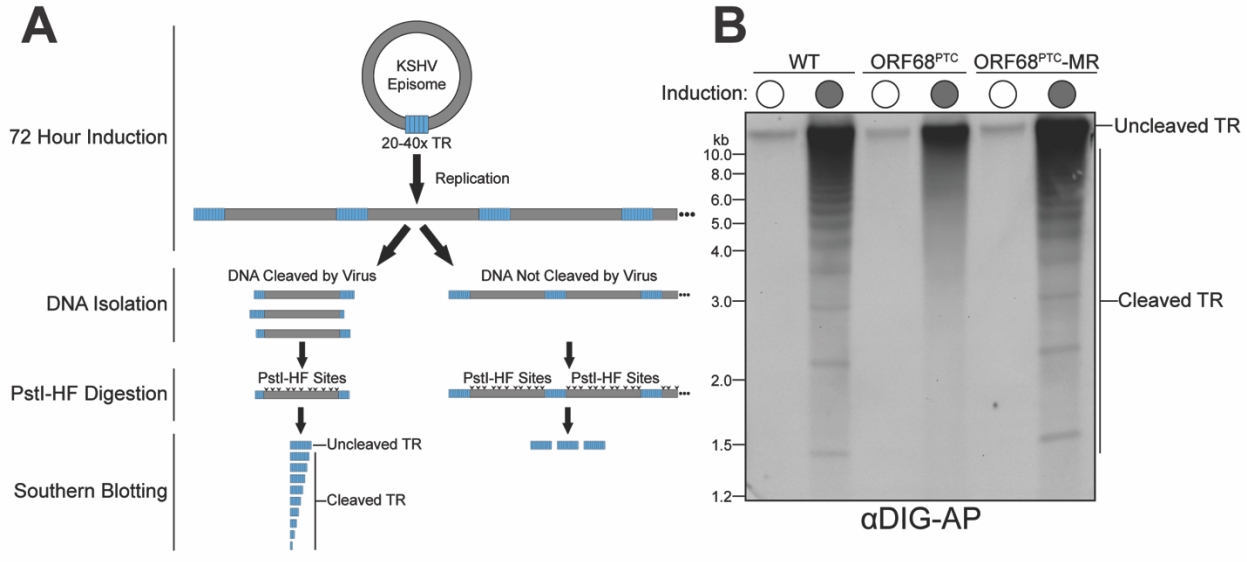

Figure 2.4. ORF68^{PTC} virus displays a genome cleavage defect. (A) Diagram depicting the DNA cleavage assay protocol and the expected TR DNA laddering phenotype (or lack thereof) upon infection with WT or ORF68^{PTC} virus. **(B)** Southern blot of the PstI-HF digested DNA with a TR probe from cells infected with WT, ORF68^{PTC}, or ORF68^{PTC}-MR virus.

KSHV ORF68^{PTC} accumulates exclusively B-capsids

During herpesvirus assembly, immature procapsids are initially formed that contain internal scaffolding proteins, which are subsequently proteolytically cleaved and extruded during the process of DNA packaging (Gibson et al.; Rixon et al., 1988). This process yields mature, DNA-containing C-capsids, but in the case of unsuccessful DNA packaging, either empty A-capsids or scaffold-containing B-capsids are formed (Tandon et al., 2015). To visualize the contribution of ORF68 towards capsid maturation, we performed transmission electron microscopy on fixed

samples of lytically-reactivated iSLK cells containing either WT or ORF68^{PTC} KSHV. In the nuclei of WT KSHV infected cells, we observed A, B, and C capsids (Figure 5a, b). In contrast, ORF68^{PTC} infected cells contained exclusively B capsids (Figure 5a, b), indicating that KSHV DNA packaging is not initiated in the absence of ORF68.

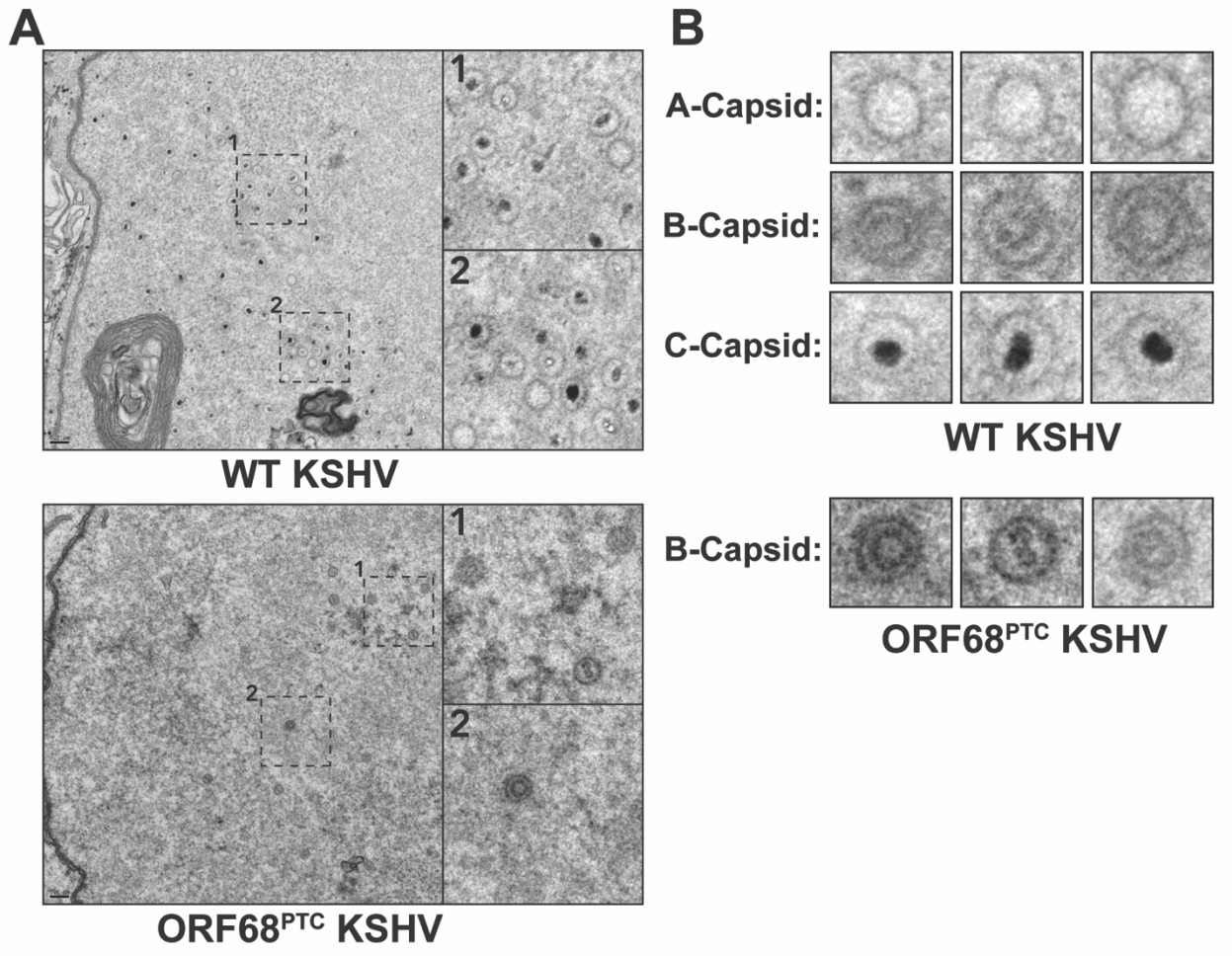

Figure 2.5. Transmission electron microscopy of WT and ORF68^{PTC} KSHV-infected cells. (A) Representative images of the nuclei of iSLK cells infected with WT or ORF68^{PTC} KSHV. Boxed regions are shown to the right at higher magnification to better visualize virion morphology. **(B)** Representative images of individual capsids observed in iSLK cells infected with WT or ORF68^{PTC} KSHV, grouped by their maturation stage. Only B-capsids were observed in cells infected with ORF68^{PTC} KSHV.

ORF68 binds DNA with high affinity *in vitro* and is associated with metal-dependent nuclease activity

In order to study the biochemical activity of ORF68 as it relates to DNA packaging, we sought to generate pure ORF68 protein. Our attempts to isolate recombinant ORF68 from *E. coli* bacteria, *Pichia pastoris* yeast, and *SF9* insect cells did not yield properly folded protein (data not

shown). Thus, we instead purified TwinStrep-tagged ORF68 from transiently transfected HEK293T cells by binding to Strep-TactinXT resin, followed by separation of ORF68 from the TwinStrep tag by PreScission protease cleavage and subsequent size exclusion chromatography (Figure 6a). Mass spectrometry of the purified sample detected ORF68 but no other contaminating proteins (data not shown). Notably, ORF68 eluted from gel filtration columns as a ~275 kDa oligomer (based on injected standards) rather than as a monomer (Figure 6b).

Given the failed DNA cleavage and packaging phenotypes associated with the ORF68^{PTC} virus, we hypothesized that ORF68 might directly bind the viral genome to help direct DNA packaging. We therefore used electrophoretic mobility shift assays (EMSA) to monitor binding of purified ORF68 to a DNA probe containing the sequence of the KSHV TR *in vitro*. Indeed, ORF68 efficiently bound DNA with an apparent K_d of (53.34 ± 2.11) nM (Figure 7a, b). The binding was cooperative, with a Hill coefficient of 1.88 ± 0.12 (Figure 7b). This is comparable to the 72 nM K_d of KSHV LANA binding to the terminal repeat (Hellert et al., 2015). Multiple higher-order binding events occurred at increased protein concentrations, resulting in several discrete bands of protein-bound DNA (Figure 7a). Although this *in vitro* DNA-binding is robust, it does not appear to be specific, as similar length probes of varying GC content from disparate sources were bound with similar affinity, and also displayed higher order binding events (data not shown).

ORF68 has no identifiable domains aside from several predicted zinc finger motifs that appear to be important for the structural integrity of the protein (Chang et al., 1996). However, we noted that in the presence of Mg^{2+}, the TR probe or other circular or linear plasmid DNA was degraded upon incubation with ORF68, suggesting that it may possess nuclease activity (Figure 7c, data not shown). Nuclease activity required metal ions for catalysis, with a preference for Mg^{2+} or Mn^{2+}, drastically reduced activity with Co^{2+} or Ni^{2+}, and no activity with Ca^{2+} or Zn^{2+} (Figure 7d). Reactions were sensitive to EDTA or similar metal-chelating agents, consistent with our observations that EDTA-containing buffers caused the precipitation of ORF68. Although our mass spectrometry analysis of purified ORF68 did not detect contaminating peptides, at present we cannot formally rule out the possibility that trace levels of a cellular nuclease co-purified with ORF68, rather than nuclease activity being an intrinsic feature of ORF68. However, given that ORF68 contains putative zinc finger motifs, we reasoned that in addition to inhibition by EDTA, the associated nuclease activity should be sensitive to the zinc-specific chelator N,N,N',N'-tetrakis(2-pyridinylmethyl)-1,2-ethanediamine (TPEN), which has high affinity for Zn^{2+} (K_d= 2.6 x 10^{-16} M), but very low affinity for Mg^{2+} (K_d= 2.6 x 10^{-2} M) and other divalent cations (Arslan et al., 1985; Golovine et al., 2008; Hyun et al., 2001). Indeed, the addition of TPEN prevented degradation of DNA in the presence of ORF68, but not DNase I, a nuclease that requires Mg^{2+} for catalysis but does not contain any structural zinc (Figure 7e). Collectively, these data demonstrate that KSHV ORF68 is a zinc finger-containing protein that can bind DNA and is associated with a zinc-dependent DNase activity.

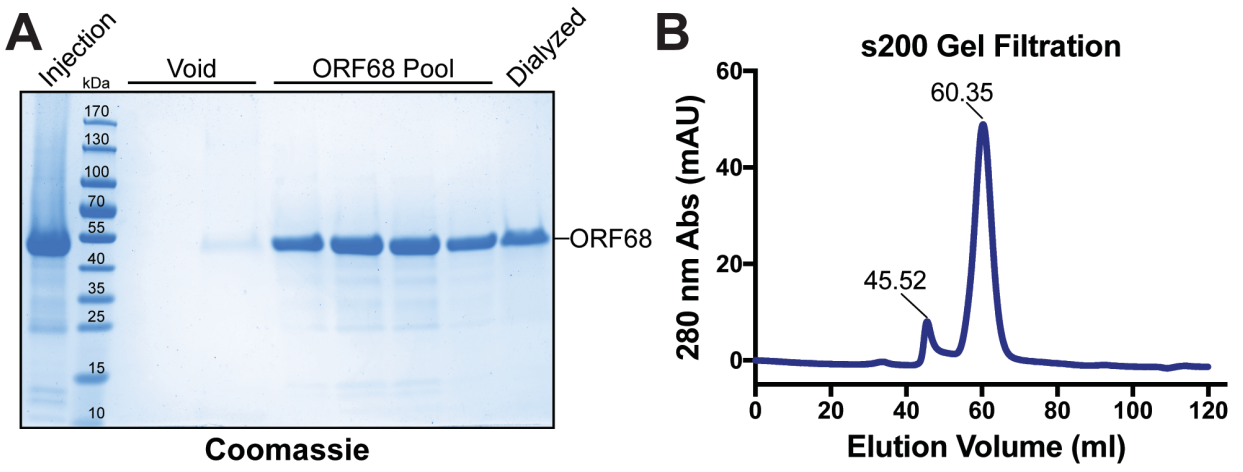

Figure 2.6. Purification of recombinant ORF68 from transiently transfected HEK293T cells. (A) Colloidal Coomassie-stained gel demonstrating the purity and molecular weight (~52 kDa) of ORF68 eluted from the s200 gel filtration column. Fractions containing ORF68 were pooled, concentrated, and dialyzed into storage buffer; a sample of which was loaded in the final lane. **(B)** Absorbance trace of the s200 gel filtration column, measured at 280 nm. The first peak represents the void elution at 45.52 ml and the second peak represents ORF68 at 60.35 ml.

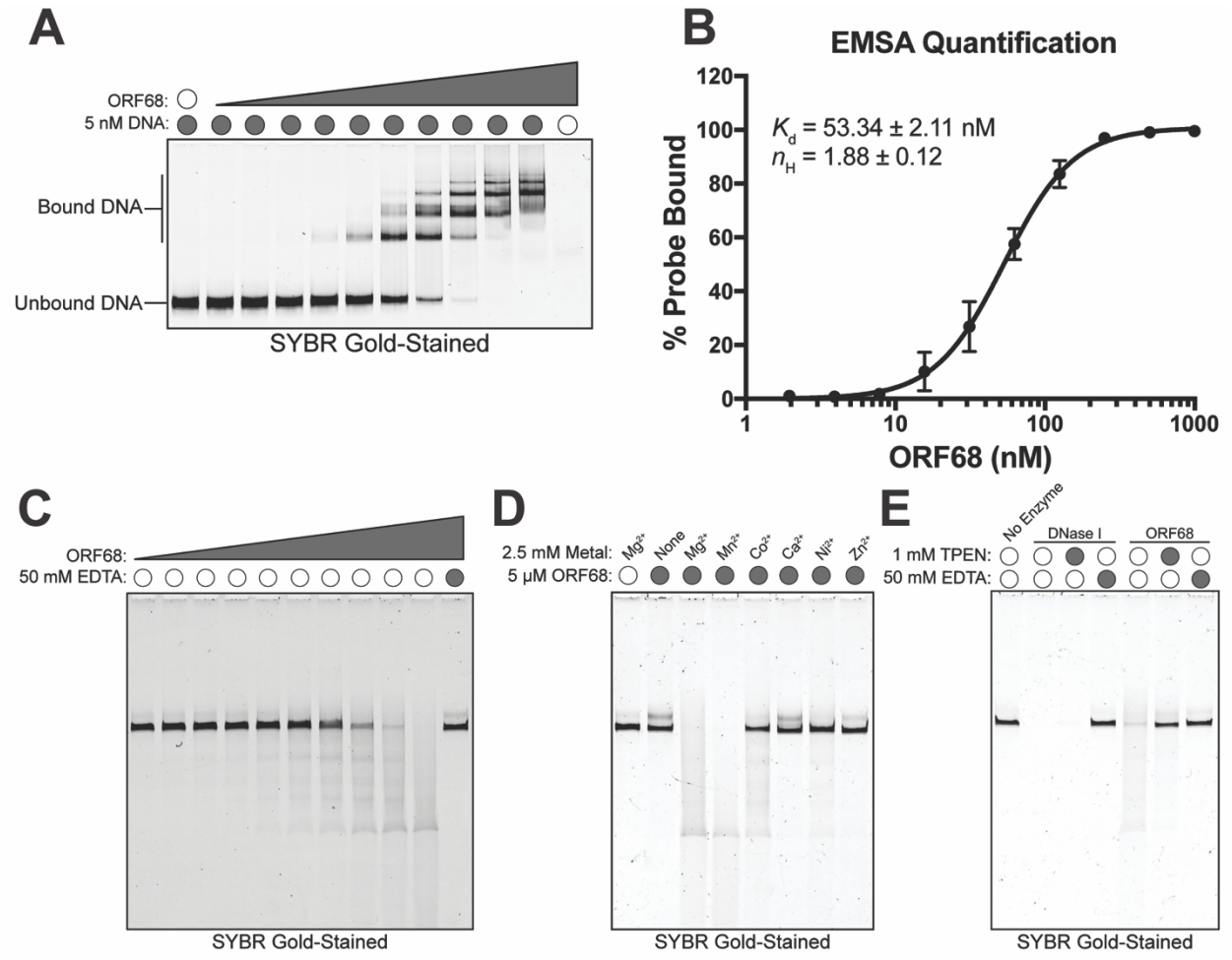

Figure 2.7. Purified recombinant ORF68 shows robust DNA binding and is associated with nuclease activity. (A) Representative EMSA showing increasing amounts of ORF68 binding to the subunit-length TR DNA probe. **(B)** Binding curve of ORF68 to DNA derived from quantification of three technical replicates of the EMSA, yielding an observed K_d of (53.34 ± 2.11) nM with a Hill coefficient of 1.88 ± 0.12. **(C)** Nuclease assay with increasing amounts of ORF68, incubated with an ~800bp TR probe in the presence or absence of EDTA. **(D)** Analysis of TR probe degradation in the presence of purified ORF68 upon addition of the indicated metal. **(E)** Gel comparing degradation of the TR probe in the presence of purified ORF68 or DNaseI +/- 1 mM TPEN or 50 mM EDTA.

Discussion

Our data firmly establish that KSHV ORF68 is essential for genome encapsidation in infected cells, and further suggest novel roles for purified ORF68 protein in DNA binding and cleavage. This is the first demonstration of direct DNA binding by a DNA packaging-associated protein in gammaherpesviruses, and the ORF68-associated nuclease activity suggests a previously unappreciated function for this protein, which may relate to viral genome processing

and encapsidation. Such a role would be consistent with the defects in viral TR cleavage, DNA packaging, and infectious virion formation we observed in cells infected with the ORF68^{PTC} virus. It is further supported by our TEM analysis of infected cells, which showed that in the absence of ORF68, DNA encapsidation was not initiated, as evidenced by the absence of A- and C-capsids. Finally, our data are in line with phenotypes observed upon deletion of the ORF68 homologs in HSV-1 (Albright et al., 2014), HCMV (Borst et al., 2008) and Epstein-Barr virus (EBV) (Pavlova et al., 2013). Indeed, in EBV, deletion of this BFLF1 gene was used to generate defective viral particles for use in vaccine development (Pavlova et al., 2013).

The ORF68 homolog in HSV-1 (UL32) was recently shown to be involved in modulation of disulfide bond formation during procapsid formation, which requires the presence of the conserved C-X-X-C motifs (Albright et al., 2014). Deletion of individual cysteines within four of the five motifs prevented complementation of a UL32 deletion mutant virus, and in the absence of UL32 the disulfide bond profiles of other viral proteins were altered. In ORF68, however, the C-X-X-C motifs appear to be important for its structural integrity, as chelation of Zn^{2+} causes ORF68 to precipitate during purification in a manner that suggests unfolding (unpublished observations). Thus, an important future challenge will be to resolve if these two functions are related, or if specific roles for UL32 and ORF68 have diverged between the alpha- and gammaherpesviruses.

In the KSHV episome, the terminal repeats are present as 20 to 40 copies of a highly repetitive ~800bp, 85% GC sequence (Juillard et al., 2016). Unlike related herpesviruses, the packaging and cleavage signals in the KSHV terminal repeats are unknown. However, by using a probe generated from the entire repeat we could capture terminal repeats of any length. In a WT KSHV infection, this yields a ladder-like cleavage pattern reflective of the fact that the genome is replicated as head-to-tail concatemers, separated by an arbitrary number of terminal repeats. While each genome should be cut only once at each end during packaging, the specific number of repeats left at each genome terminus is variable (Tong and Stow, 2009; Varmuza and Smiley, 1985). This is in contrast to viruses lacking ORF68, which displayed WT levels of DNA replication by both qPCR and Southern blotting, but no apparent resolution of the amplified concatemers into unit-length genomes. These data reinforce the hypothesis that KSHV ORF68 is not required for genome replication but is integral to the process of DNA encapsidation. Interestingly, a recent cryo-electron microscopy (cryoEM) structure of the HSV-1 portal-vertex shows a pentameric assembly associated with the portal complex (McElwee et al., 2018). Given that KSHV ORF68 purifies as an oligomer that is roughly the size of a pentamer, one possibility is that this cryoEM-visualized pentameric assembly may serve as an interaction site for ORF68 during the DNA packaging reaction.

Given the stage at which ORF68^{PTC} virus fails during virion maturation, we hypothesized that ORF68 may interact with the viral genome to promote DNA packaging. Indeed, purified ORF68 robustly bound the prototypical terminal repeat subunit, with an observed K_d of ~50nM. This is comparable to the strength of the TR interaction for the KSHV latency-associated episome tethering protein LANA, strongly suggesting that viral DNA binding is a biologically relevant feature of ORF68 (Hellert et al., 2015). However, it is important to note that *in vitro*, the DNA binding activity of ORF68 does not have apparent sequence specificity. In cells, it is possible that sequence specificity is conferred by other viral (or cellular) factors. It is also possible that the DNA

binding activity participates in a distinct facet of the viral replication cycle, although we did not detect any defects in the ORF68^{PTC} virus prior to encapsidation. The ~800bp terminal repeat subunits are somewhat long for traditional EMSA probes and as such, multiple binding events could be observed. Furthermore, binding of ORF68 to DNA was cooperative, as is frequently observed for DNA binding proteins (Siggers and Gordan, 2014). This cooperativity may indicate that ORF68 binds the DNA probe at multiple sites, that the binding of the first ORF68 molecule alters the DNA conformation in a way that promotes additional ORF68 binding, or simply reflect our observation that ORF68 exists as an oligomer in solution.

In addition to DNA binding, we made the unexpected observation that in the presence of the divalent cations Mg^{2+} or Mn^{2+}, incubation with ORF68 caused degradation of DNA. These cations are commonly used by nucleases (Yang, 2010), and future studies are aimed at exploring residues in ORF68 that could serve to coordinate divalent cations. Our robust purification scheme, coupled with the absence of any detectable co-purifying peptides by mass spectrometry and the fact that addition of the zinc-chelator TPEN specifically blocked ORF68-associated nuclease activity suggest that the activity is intrinsic to ORF68. However, aside from the zinc finger motifs, no predicted domains or structural information is currently available for ORF68. Thus, a key challenge will be to establish if and how ORF68 promotes DNA cleavage in cells. Formal proof of nuclease activity will ultimately require structural data to identify putative catalytic domain(s), which should enable isolation of point mutants to be tested for DNA cleavage. Similar to the DNA binding activity, our *in vitro* cleavage reactions do not capture TR-specific targeting, as we found that other non-viral DNA was similarly susceptible to ORF68-associated degradation (unpublished observations). This might suggest that other components of the packaging machinery are required to confer specificity or, alternatively, that the putative nuclease activity is involved in an ORF68 function independent of DNA encapsidation.

While seven herpesviral proteins are required for proper DNA encapsidation, only two have been shown to directly act on DNA. A crystal structure of a fragment of the HSV-1 UL15 terminase motor protein, which is homologous to KSHV ORF29, revealed that it adopts an RNase H-like fold and possess non-specific DNA nicking *in vitro* (Nadal et al., 2010; Selvarajan Sigamani et al., 2013). Purified HSV-1 UL28, another terminase motor protein and the homolog of KSHV ORF7, has also been shown to bind terminal repeat DNA *in vitro* (Adelman et al., 2001). It has high specificity for certain terminal repeat DNA probes, but only after heat treatment of the DNA, which causes them to adopt non-duplex structures (Adelman et al., 2001). This suggests that the UL28-DNA interaction is structure dependent, in contrast to KSHV ORF68, which bound duplex DNA with no apparent sequence specificity or requirement for higher order structures. Whether the UL15 and UL28 functions are conserved in their KSHV homologs ORF29 and ORF7, and how KSHV ORF68 mechanistically contributes to DNA encapsidation remains to be established.

Finally, although the majority of ORF68 is concentrated in replication compartments, the protein also localizes within discrete puncta in the cytoplasm, as well as in larger aggregates adjacent to the nucleus. While we hypothesize that the larger structures represent unfolded protein in aggresomes, the smaller punctate structures are suggestive of a distinct function for ORF68 in the cytoplasm, possibly unrelated to its role in packaging. Notably, HSV-1 UL32 was also shown to localize to the cytoplasm, particularly late in infection, where it forms perinuclear foci

(Albright et al., 2014). Given the frequently multifunctional roles of viral proteins, it will be of interest to explore possible additional cytoplasmic activities of ORF68.

Materials and Methods

Plasmids

TwinStrep-PreScission-ORF68 was cloned into the pHEK293 UltraExpression I vector (Clontech) digested with XhoI and SalI. ORF68 was amplified with the primers 5'-TGGAATTCTGCAGATATGTTTGTTCCCTGGCAACTCG-3' and 5'-GCCACTGTGCTGGATTCAAGCGTACAAGTGTGACGTCT-3' while TwinStrep-PreScission was amplified using the primers 5'-CCTCCCCGGGCTCGAATGAGTGCGTGGAGTCATCCTCAATTCGAGAAAGGTG-3' and 5'-GGGCCCCTGGAACAGAACTTCCAGTCCGGATTTTTCGAACTGCGGG-3'. The two fragments were first assembled by PCR and then inserted into the vector by InFusion cloning (Clontech).

ORF68 and ORF68-Extended were cloned into pCDNA4 (ThermoFisher) digested with EcoRV using 5'-TGGAATTCTGCAGATATGTTTGTTCCCTGGCAACTCG-3' for ORF68, 5'-TGGAATTCTGCAGATATGTCACGAGGCAGAAGCTGG-3' for ORF68-Extended, and 5'-GCCACTGTGCTGGATTCAAGCGTACAAGTGTGACGTCT-3' as the reverse primer for both. PCR products were inserted into the vector using InFusion cloning.

Cell Lines

HEK293T (ATCC CRL-3216) cells were maintained in DMEM +10% FBS. HEK293T-ORF68 cells were maintained in DMEM + 10% FBS, 325 µg/ml zeocin. iSLK.BAC16 (Brulois et al., 2012) cells were maintained in DMEM + 10% FBS, 1 mg/ml hygromycin B, and 1 µg/ml puromycin. TREx-BCBL1 (Nakamura et al., 2003) cells were maintained in RPMI 1640 + 20% FBS.

Viral mutagenesis and infection studies

The KSHV ORF68 Premature Termination Codon (ORF68^{PTC}) mutant and corresponding mutant rescue (MR) were engineered using the scarless Red recombination system in BAC16 GS1783 *E. coli* as previously described (Brulois et al., 2012), except using two gBlocks (IDT) to introduce the mutation. Each gBlock contained half of the kanamycin resistance cassette, as well as the desired mutation, and were joined by short overlap extension PCR before being used as the linear insert in the established protocol.

The BAC16 ORF68 mutant and MR were purified using the NucleoBond BAC 100 kit (Clontech). iSLK cell lines latently infected with the KSHV ORF68^{PTC} virus were then established by co-culture of the relevant BAC16-containing HEK293T cells with uninfected target iSLK-Puro cells. HEK293T cells constitutively expressing ORF68 (HEK293T-ORF68) were transfected with 12 µg of BAC16 containing ORF68^{PTC} or MR using linear polyethylenimine (PEI, MW ~25,000) at a 1:3 DNA:PEI ratio. The following day, the cells were trypsinized and mixed 1:1 with iSLK-puro cells, then treated with 30 nM 12-O-Tetradecanoylphorbol-13-acetate (TPA) and 300 nM sodium butyrate for 4 days to induce lytic replication. Cells were then incubated with selection media containing 300 µg/ml hygromycin B, 1 µg/ml puromycin, and 250 µg/ml G418. Media was

replaced every other day for ~2 weeks, gradually increasing the hygromycin B concentration to 1 mg/ml until there were no HEK293T cells remaining and the iSLK cells were green and replicating.

For induction studies, BAC16-containing iSLK cells were treated with 1 μg/ml doxycycline and 1 mM sodium butyrate, and TREx-BCBL1 cells were induced with doxycycline (1 μg/ml) and TPA (25 ng/ml) for the indicated amount of time. Virion production from reactivated iSLK cells was measured using supernatant transfer assays at 72 hours post induction. The supernatant was filtered through a 0.45 μM PES filter, then 2 ml were mixed with $1x10^6$ freshly trypsinized HEK293T cells. The cell mixture was placed into a 6 well plate and centrifuged at 1,200 x *g* for 2 hours at 32˚C. The following day, cells were trypsinized, fixed in 4% paraformaldehyde, then analyzed for GFP expression by flow cytometry (BD Csampler, BD Biosciences). Data was analyzed using FlowJo v10.

Generation of HEK293T cells stably expressing ORF68

HEK293T-ORF68 cells were generated by cloning ORF68 into pLJM1 (a gift from David Sabatini (Addgene plasmid #19319) (Sancak et al., 2008)) in which the puromycin resistance had been exchanged for zeocin. The vector was digested with AgeI and EcoRI (New England Biolabs) and ORF68 was amplified by PCR using primers 5'-CGCTAGCGCTACCGGATGTTTGTTCCCTGGCAACTCGG-3' and 5'-TCGAGGTCGAGAATTTCAAGCGTACAAGTGTGACGTCTG-3' and inserted using T4 DNA Ligase (NEB). 1.6 μg of this plasmid was co-transfected into HEK293T cells along with the lentiviral packaging plasmids pMD2.G (0.5 μg) and psPAX2 (1.3 μg) (gifts from Didier Trono (Addgene plasmid #12259 and #12260)) using PEI. 48 hours after transfection, the supernatants were collected, filtered through a 0.45 μm PES filter, diluted 1:4 (supernatant:media) in DMEM containing 8 μg/ml of polybrene, and added to the wells of a 6 well plate containing $1x10^6$ HEK293T cells per well. The plates were centrifuged for 2 hours at 1,200 x *g* (32˚C), incubated overnight, and the media replaced with fresh DMEM (10% FBS) containing 325 μg/ml zeocin until no further cell death was observed, roughly two weeks.

Western blots and antibody production

Cells were lysed in protein lysis buffer (50 mM Tris-HCl pH 7.6, 150 mM NaCl, 3 mM $MgCl_2$, 10% glycerol, 0.5% NP-40, cOmplete EDTA-free Protease Inhibitors [Roche]) and clarified by centrifugation at 20,000 x *g* for 10 min at 4˚C. Lysates were resolved by SDS-PAGE and western blotted with rabbit anti-ORF68 (1:5000), rabbit anti-ORF59 (1:10,000), rabbit anti-K8.1 (1:10,000), rabbit anti-histone H3 (1:3000, Cell Signaling 4499S), or mouse anti-GAPDH (1:5000, Abcam ab8245). Rabbit anti-ORF68, -ORF59, and -K8.1 was produced by Pocono Rabbit Farm & Laboratory by immunizing rabbits against MBP-ORF68, -ORF59, or -K8.1 (gifts of Denise Whitby, (Labo et al., 2014)). Sera was harvested and used directly for ORF59 and K8.1, while ORF68-specific antibodies were isolated by first collecting antibodies that bound an MBP-ORF68 column, followed by removal of non-specific antibodies on an MBP column. Both selection columns were generated using the AminoLink Plus Immobilization Kit (ThermoFisher).

Immunofluorescence assays

Cells were fixed with 4% paraformaldehyde in PBS, permeabilized with ice-cold methanol at -20˚C for 20 min, then blocked with BSA blocking buffer (PBS, 1% Triton X-100, 0.5% Tween20, 3% BSA) for 30 minutes at room temperature. They were then incubated with rabbit anti-ORF68 and mouse anti-ORF59 (Advanced Biotechnologies) antibodies (diluted 1:100 in blocking buffer) overnight at 4˚C, washed with PBS, and incubated with secondary antibody (AlexaFluor594 or DyLight650, 1:1000 in BSA blocking buffer) for 1 h at 37˚C, and mounted using VectaShield HardSet with DAPI (ThermoFisher). Images were acquired on an EVOS FL inverted fluorescent microscope (ThermoFisher).

DNA isolation and qPCR

iSLK-BAC16 cells were incubated with 5x proteinase K digestion buffer (50 mM Tris-HCl pH 7.4, 500 mM NaCl, 5 mM EDTA, 2.5% SDS) and digested with proteinase K (80 µg/ml) overnight at 55˚C. The gDNA was isolated using Zymo Quick gDNA Miniprep Kit according to the manufacturer's instructions.

Quantitative PCR was performed on the isolated DNA using iTaq Universal SYBR Green Supermix on a QuantStudio3 Real-Time PCR machine. DNA levels were quantified using relative standard curves with primers specific for KSHV ORF57 (5'-GGTGTGTCTGACGCCGTAAAG-3' and 5'-CCTGTCCGTAAACACCTCCG-3') or a region in the GAPDH promoter (5'-TACTAGCGGTTTTACGGGCG-3' and 5'-TCGAACAGGAGGAGCAGAGAGCGA-3'). The relative genome numbers were normalized to GAPDH to account for loading differences and to uninduced samples to account for starting genome copy number.

Protein purification

TwinStrep-PreScission-ORF68 was transfected using PEI into 50 90% confluent 15 cm plates of HEK293T cells for 48h. Cells were lysed in 5 ml of lysis buffer (100 mM Tris-HCl pH 8.0, 300 mM NaCl, 1 mM DTT, 5% glycerol, 0.1% CHAPS, 1 µg/ml avidin, cOmplete EDTA-free protease inhibitors [Sigma-Aldrich]) per 1 g of cell pellet and rotated at 4˚C for an additional 30 minutes. The viscosity was reduced by sonication, whereupon debris was removed by centrifugation at 20,000 x *g* (4˚C) for 30 min followed by filtration through a 0.45 µm PES filter with a glass pre-filter (Millipore). Lysate was passed three times over a gravity column containing Strep-Tactin XT Superflow slurry (IBA) then washed with 5 column volumes of strep running buffer (100 mM Tris-HCl pH 8.0, 300 mM NaCl, 1 mM DTT, 5% glycerol, 0.1% CHAPS). ORF68 was eluted by rotating the column overnight in HRV 3C Protease (Millipore) at a 1:100 Protease:ORF68 ratio in buffer containing 2 mM DTT, then concentrated to ~500 µL using a 30 kDa cut-off Centriprep spin concentrator (Millipore). The concentrated eluate was centrifuged at 20,000 x *g* for 10 min to remove precipitates and injected onto a HiLoad 16/600 Superdex 200 pg gel filtration column (GE Healthcare), previously equilibrated with Gel Filtration buffer (50 mM HEPES pH 7.6, 100 mM NaCl, 100 mM KCl, 5% glycerol, 0.1% CHAPS). Gel filtration was performed using an AKTA Pure FPLC (GE Healthcare). Fractions resulting from the gel filtration were analyzed by SDS-PAGE and staining with colloidal Coomassie (Dyballa and Metzger, 2009). Fractions containing ORF68 were pooled and concentrated as before, until the total concentration was ~2 mg/mL as evaluated by absorbance at 280 nm. The concentrated protein was injected into a 20 kDa cut-off Slide-A-Lyzer

dialysis cassette (ThermoFisher) and dialyzed against storage buffer (Gel Filtration buffer lacking CHAPS). Dialyzed protein was diluted to 1 mg/ml, aliquoted, and snap-frozen in liquid nitrogen before being stored at -80˚C.

Electrophoretic mobility shift assay (EMSA)

Single-subunit terminal repeat DNA probes were generated by digesting pK8TR (a gift of the Kaye lab (Habison et al., 2017)) with AscI overnight. The resulting cleavage products were separated on an agarose gel and the 800 bp band was excised, isolated from agarose, and purified further by phenol:chloroform extraction and ethanol precipitation.

EMSA assays were assembled on ice in gel shift buffer (25 mM HEPES pH 7.6, 50 mM NaCl, 50 mM KCl, 0.1 mg/ml BSA, 0.05% CHAPS, 10% glycerol) with 5 nM probe and 2-fold dilutions of ORF68 ranging from 1.95 nM to 1000 nM. Once assembled, the reactions were incubated at 30˚C for 30 minutes. Samples were directly loaded onto a 3.5% 29:1 polyacrylamide:bisacrylamide native gel containing 45 mM Tris-borate pH 8.3, 10% glycerol, which was degassed thoroughly before polymerization. Samples were separated by electrophoresis at 250V for 1 hour at 4˚C in pre-chilled 0.5x TB (45 mM Tris-borate pH 8.3). Tris-borate buffer was used in lieu of TBE because ORF68 precipitates in the presence of EDTA. The native polyacrylamide gel was cast to a final concentration of 0.5x Tris-borate, 10% glycerol, and was degassed thoroughly before polymerization. Following the electrophoresis, the gel was removed from the running cassette and stained with SYBRgold (ThermoFisher) in 0.5x TB for 30 minutes, rocking at room temperature and protected from light. Staining solution was removed by briefly washing with fresh 0.5x TB and the gel was imaged on a ChemiDoc Touch (Bio-rad). All bands were quantified using ImageLab v6.0 (Bio-rad) and percent bound probe was determined by dividing shifted band intensity by the total intensity of all bands in that lane. Binding curves were generated using Prism v7 (GraphPad) by non-linear regression fit using least-squares. Shown data represents three technical replicates performed on different days.

Nuclease assays

The EMSA probe was also used for nuclease assays and was produced as described above. Reactions were assembled in nuclease buffer (25 mM HEPES pH 7.6, 50 mM NaCl, 50 mM KCl, 0.1 mg/ml BSA, 2.5 mM $MgCl_2$) with 1 nM DNA probe and 2-fold dilutions of ORF68 ranging from 9.77 to 5000 nM. The reactions were incubated at 37˚C overnight. The following day, reactions were quenched using stop buffer (4 M urea, 50 mM EDTA, 1 mM $CaCl_2$, 0.8 U proteinase K [New England Biolabs], 1x Purple Loading dye [New England Biolabs]; final concentrations) and incubating at room temperature for 30 minutes. The samples were then loaded onto a denaturing polyacrylamide gel (8 M Urea, 4.5% 29:1 acrylamide:bisacrylamide, 90 mM Tris-borate pH 8.3, 2 mM EDTA, degassed before polymerization), which had been pre-run at 200V for 30 minutes in 1x TBE to evenly heat the gel. The samples were separated at 200V for 45 minutes before being removed from the running cassette and stained with SYBRgold in 1X TBE for 30 minutes at room temperature, protected from light. Gels were visualized using a ChemiDoc Touch (Bio-Rad). Metal-dependence tests were performed as described but changing the 2.5 mM $MgCl_2$ to the chloride salts of the indicated divalent cations. TPEN-treatment was performed as described but protein was treated with either TPEN in 100% ethanol (1 mM), mock treated with

100% ethanol, or EDTA (50 mM) for 10 minutes on ice prior to adding the DNA substrate. DNaseI (New England Biolabs) was diluted to 0.02U in ORF68 storage buffer before addition to reactions.

Southern blotting

BAC16.iSLK cells were harvested in proteinase K digestion buffer and incubated overnight with proteinase K (80 µg/ml). DNA was isolated by phenol:chloroform extraction and ethanol precipitation, then resuspended in TE buffer. DNA (10 µg) was digested with PstI-HF (New England Biolabs) overnight then separated by electrophoresis in a 0.7% agarose 1x TBE gel stained with SYBRsafe. The DNA was transferred to a NYTRAN-N membrane (GE Healthcare) by capillary action in 20x SSC overnight and crosslinked to the membrane in a StrataLinker 2400 (Stratagene) using the AutoUV setting.

The membrane was treated according to the DIG High Prime DNA Labeling and Detection Starter Kit II (Roche) following the manufacturer's instructions. Briefly, the membrane was hybridized at 42˚C in EasyHyb Buffer with a DIG-labeled linear terminal repeat subunit derived from AscI (New England Biolabs) digested pK8TR, which was labeled according to kit instructions. Following overnight hybridization, the membrane was washed twice with 2x SSC (+0.1% SDS) at room temperature and then twice with 0.5x SSC (+0.1% SDS) at 68˚C. Using supplied reagents, the blot was then blocked, incubated with anti-DIG-AP antibody, and visualized on a ChemiDoc Touch (Bio-Rad).

Electron microscopy

iSLK.BAC16 WT or ORF68^{PTC}-infected cells were induced for 48 hours as described above. Cells were washed once with PBS and fixed with 2% glutaraldehyde, 4% paraformaldehyde in 100 mM sodium cacodylate buffer, pH 7.2 for 10 minutes at room temperature. Fixative was removed and cells were scraped into 2% glutaraldehyde in 100 mM sodium cacodylate buffer, pH 7.2 and evenly resuspended by pipetting. Cells were then washed with 1% osmium tetroxide, 0.8% ferricyanide in 100 mM sodium cacodylate buffer, pH 7.2, before being treated with 1% uranyl acetate and dehydrated with increasing concentrations of acetone. Samples were then infiltrated and embedded in resin, from which 70 nm sections were cut on a Reichert-Jung microtome. Sections were picked up on copper mesh grids coated with 0.5% formvar, post-stained with uranyl acetate and lead citrate, and examined using an FEI Tecnai 12 transmission electron microscope.

Acknowledgements

We thank all members of the Glaunsinger and Coscoy labs, in particular Angelica Castañeda and Allison Didychuk, as well as Dr. Sandra Weller for their helpful suggestions and critical reading of the manuscript. We also thank Reena Zalpuri and all of the staff at the University of California Berkeley Electron Microscope Laboratory for advice and assistance in electron microscopy sample preparation and data collection. B.G. is an investigator of the Howard Hughes Medical Institute. This research was also supported by NIH R01AI122528 to B.G.

Chapter 3: Kaposi's sarcoma-associated herpesvirus encodes a proteasome activator mimic that is required for infectious virion production

Introduction

Despite being recently discovered compared to the other human herpesviruses, there is a large body of work on how KSHV controls the cell during infection (Ganem, 2006). In particular, a great deal of effort has been put into understanding how KSHV controls the stability of mRNA (Bagnéris et al., 2011; Glaunsinger and Ganem, 2004), transcription (Abernathy et al., 2015; Naranatt et al., 2004), translation (Kuang et al., 2011), ubiquitination (Ashizawa et al., 2012), post-transcriptional modifications (Chang et al., 2016; Hesser et al., 2018), immune surveillance (Coscoy, 2007), and cellular pathways as a whole (Davis et al., 2015b). However, it is still unclear how KSHV controls the proteome during infection. Given the intense regulation at other stages of gene expression, it would be surprising if KSHV only controlled protein homeostasis on a protein-by-protein basis. There are many examples of this kind of targeted protein manipulation by KSHV, such as the specific removal of MHCI from the cell surface by the K3 protein. This protein contains a PHD domain, which is structurally similar to ubiquitin ligase domains, and causes the internalization and lysosomal-targeting of MHCI (Lorenzo et al., 2002). Similarly, it has been shown that the protein responsible for lytic reactivation of KSHV, ORF50 or RTA, possesses E3 ubiquitin ligase activity that targets a number of proteins to the proteasome for degradation (Yu et al., 2005). KSHV does not entirely rely on ubiquitin ligases however, as the latent protein LANA, which also tethers the viral episome to the host genome during latency, directly interfaces with the proteasome. LANA is a large protein with a repetitive central domain rich in Glu, Gln, and Asp, that is not efficiently processed by the proteasome. This property causes the proteasome to stall after it has already engaged LANA, preventing it from further degrading it or other proteins. Combined with the other described activities of LANA, this can subvert the presentation of immunogenic MHCI peptides and evade the host immune response (Kwun et al., 2011).

At the core of protein turnover in mammalian cells is the proteasome, a large, ATP-protease that plays a role in numerous cellular processes. First and foremost, it is responsible for the majority of protein degradation in mammalian cells through the ubiquitin-proteasome system (UPS). In this system, proteins to be degraded are covalently marked with a small protein called ubiquitin, often as chains of four ubiquitin molecules linked together, and are then trafficked to the proteasome. There, the proteins are engaged by the proteasome, processively unfolded, and degraded (Yedidi et al., 2017). During this process the ubiquitin chains are removed and can be recycled back into the system (Worden et al., 2017). The proteasome is made up of several subcomplexes, which perform different roles during protein degradation. The actual proteolytic machinery is sequestered in the lumen of the 20S core peptidase, which is made up of four axially-stacked heteroheptameric rings that form a barrel-shaped complex. Entry into the core peptidase is mediated by two "gates" on either end of the barrel that are natively occluded, but can open following the binding of a proteasome activator (Kish-Trier and Hill, 2013). This is usually mediated through a gate opening motif, often observed to follow the pattern of

Hydrophobic-Tyrosine-Any amino acid, or HbYX (Bard et al., 2018). In this way, the very promiscuous protease activities of the 20S are sequestered away from the general cellular environment, allowing for both broad activity and substrate specificity.

The most well-studied proteasome activator in mammalian cells is the 19S regulatory particle (RP), which is the canonical proteasome activator of the UPS (Bard et al., 2018). However, mammalian cells encode many more proteasome activators, which remain largely mysterious. What is known, is that these alternative proteasome activators can alter the substrates that the 20S core peptidase encounters and can therefore fine tune the proteome of the host cell (Stadtmueller and Hill, 2011). This presents an attractive target for a pathogen with a vested interest in controlling the host proteome, as the 20S has very little substrate specificity once a target reaches its lumen. In this vein, it has been observed that chemical inhibition of the proteasome drastically reduces KSHV virion production independent of cell death, indicating a reliance on proteasome activity for the KSHV replication cycle (Saji et al., 2011).

Given these observations, we were intrigued by the observation that KSHV ORF68 associated with multiple subunits of the proteasome (Davis et al., 2015b). We were able to confirm and further characterize this interaction, revealing that ORF68 and its homologs contain an HbYX gate opening motif that is involved in protein turnover and is required for KSHV virion production. Immunofluorescence experiments additionally revealed that the proteasome is concentrated in viral replication compartments with ORF68 (Gardner and Glaunsinger, 2018). Together, these data suggest that ORF68 may act to directly manipulate the 20S proteasome, which would represent a novel strategy for viral control of the host proteome.

Results

A KSHV ORF68-proteasome interaction is predicted by the KSHV interactome and confirmed in infected cells.

The KSHV interactome aimed to encompass all host-viral protein-protein interactions that occur in mammalian cells. This was accomplished through a series of affinity purification and mass spectrometry experiments (Davis et al., 2015b). Although a lower confidence interaction, ORF68 was found to associate with multiple subunits of the proteasome. This is more likely to be a true interaction because ORF68 was found to co-purify with 14 subunits of the proteasome, instead of just one or two (Figure 1a). To confirm that this interaction occurred, co-immunoprecipitation and western blot experiments were performed in cells transfected with a tagged unit of the proteasome, β4, which incorporates into the 20S core. Once incorporated into proteasomes, the tagged subunit can be used to recover intact proteasomes, which can be seen by the co-purification of the 20S subunit β7. Using this strategy, we found that ORF68 was robustly associated with proteasomes, but another KSHV protein used as a negative control, ORF59, was not (Figure 1b). To confirm that this was not an artifact of transient overexpression, native proteasomes were isolated from infected cells using beads conjugated with the UBL domain of RAD23, a proteasome-associated protein. Under these conditions, intact, native 26S proteasomes were isolated, as shown by the co-purification of subunits in the 20S core (β7) and 19S regulatory particle (RPT6, RPN11). ORF68 was again co-purified with proteasomes, although less robustly (Figure 1c).

ORF68 has previously been shown to concentrate in replication compartments during infection, where it plays a role in the packaging of viral DNA into nascent capsids (Gardner and Glaunsinger, 2018). To see if the proteasome is also localized to replication compartments during infection, immunofluorescence assays were performed on infected cells. During the lytic cycle, proteasomes were observed throughout the cell, but particularly in the lobed replication compartments within the nucleus. Here, proteasomes showed some co-localization with ORF68, although both proteins had extensive non-overlapping signals (Figure 2a). In contrast, during the latent cycle, proteasomes are dispersed throughout the cell, except in the nucleolus (Figure 2b).

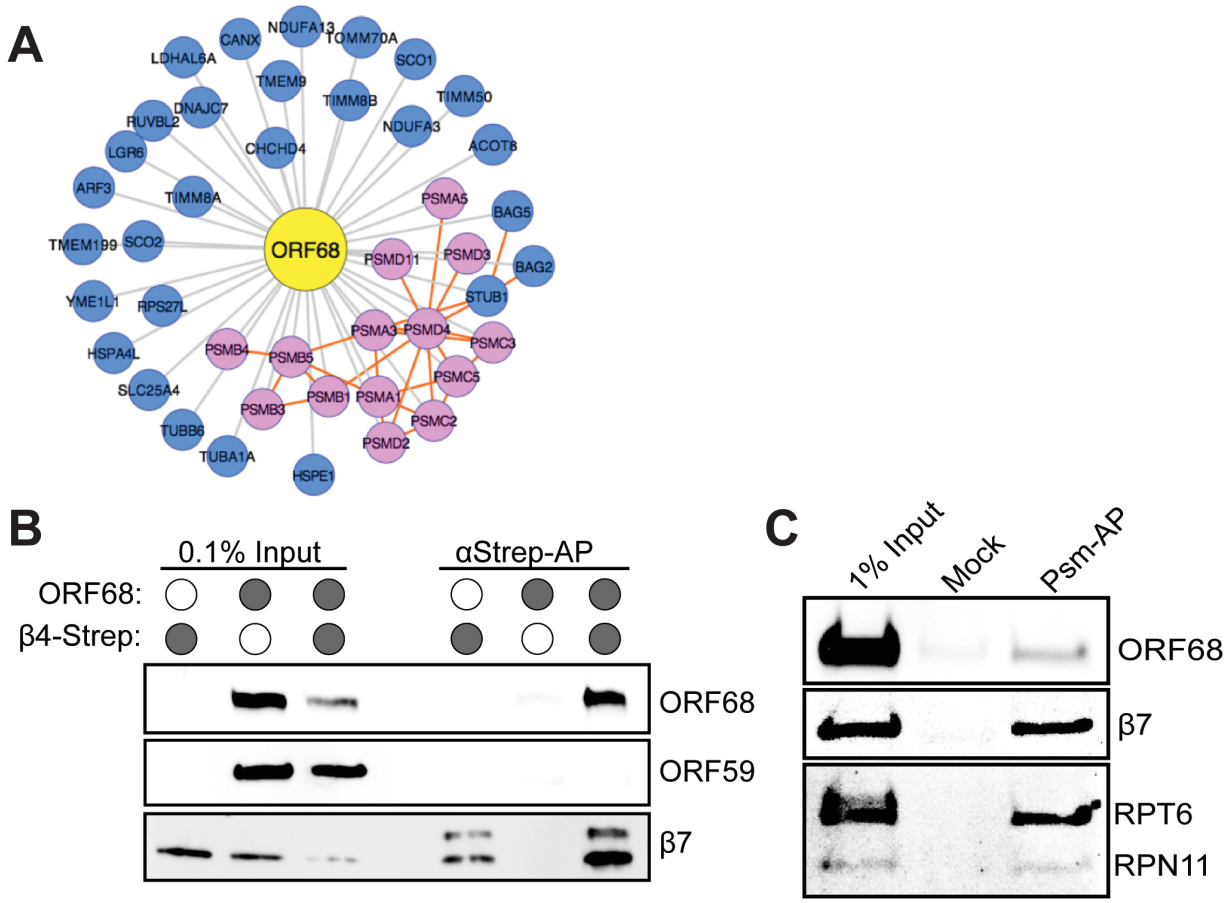

Figure 3.1. ORF68 is associated with proteasomes in mammalian cells. (A) Interaction network of ORF68 affinity purified from mammalian cells, with proteasome subunits (pink) and other host proteins (blue). Grey edges show interactions identified in the KSHV interactome, orange edges show known associations. **(B)** Co-IP western blot of proteasomes purified from HEK293T cells expressing a TwinStrep-tagged β4. ORF68 co-purifies with the proteasome, but not with control beads. ORF59 was not predicted to interact with the proteasome by the interactome and does not co-purify. β7 is a 20S subunit, showing that intact proteasomes are being isolated **(C)** Co-IP western blot of native proteasomes from infected cells showing that ORF68 co-purifies with proteasomes from infected cells. RPT6 and RPN11 are subunits of the 19S regulatory particle, demonstrating the isolation of 26S proteasomes.

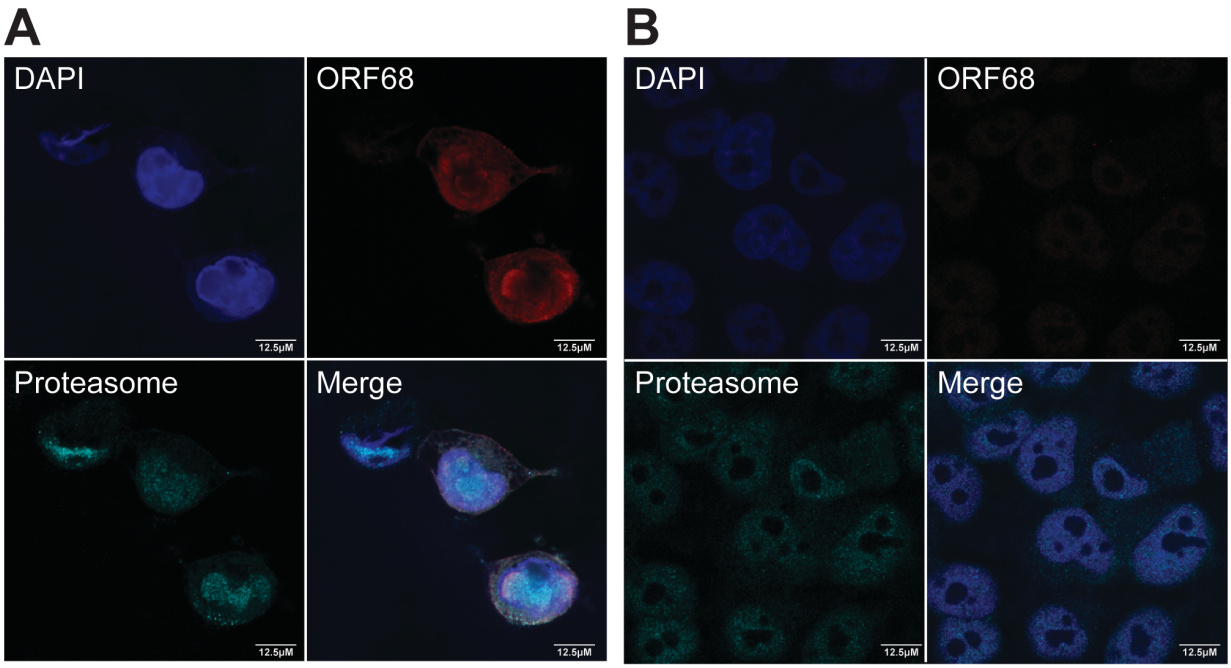

Figure 3.2. The proteasome is condensed into replication compartments, along with ORF68, during lytic KSHV infection. Reactivated **(A)** and unreactivated **(B)** iSLK BAC16 cells stained with antibodies to ORF68 (red) and the proteasome (cyan), as well as DAPI (blue). Replication compartments can be seen as lobed nuclear structures in **(A)** that are poorly stained by DAPI. Poorly-stained, but non-lobed, structures in **(B)** are nucleoli.

KSHV ORF68 contains a canonical HbYX gate opening motif that is dispensable for proteasome interaction.

Proteasome activators generally contain "gate opening" motifs, which are carboxyl-terminal motifs that open the normally closed pore of the 20S, allowing substrates to reach the protease sites. This motif generally takes the amino acid form of hydrophobic-tyrosine-any (HbYX) (Bard et al., 2018). A ClustalOmega alignment of ORF68 and homologous proteins from the other seven human herpesviruses showed that they all contain a penultimate Tyrosine, the most critical part of the HbYX motif. Furthermore, ORF68 has the sequence "LYA" which is similar to that of 19S proteasome subunits (Figure 1a).

To determine if this gate opening motif is required for the ORF68-proteasome interaction, two mutants were made, one in which the LYA motif is deleted (ORF68ΔLYA), and one in which the motif is masked by a TwinStrep tag (ORF68-TS). Gate opening motifs must be at the very carboxyl-terminus of the protein in question and can therefore be destroyed by subtraction or addition of amino acids. These mutants were used in co-immunoprecipitation assays, which revealed that the gate opening motif was not required for interaction with the proteasome (Figure 3b).

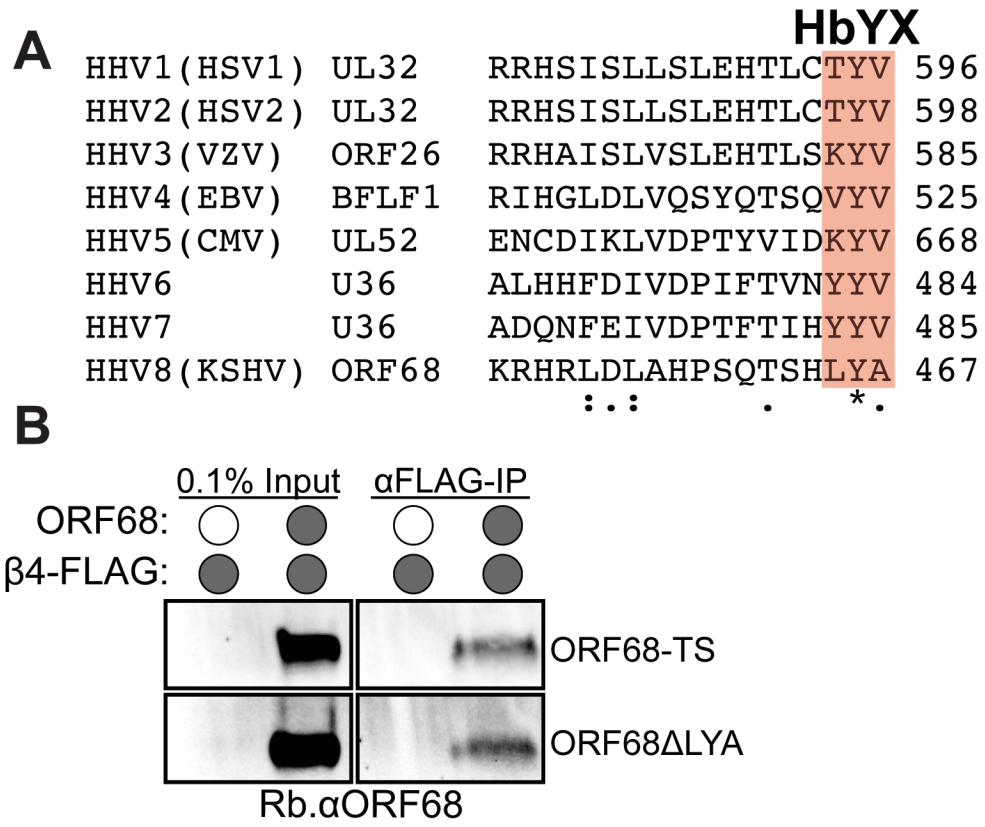

Figure 3.3. KSHV ORF68 and homologous proteins in other herpesviruses contain a HbYX gate opening motif that is dispensable for proteasome interaction. (A) ClustalOmega alignment of the carboxyl-termini of ORF68 homologs, with the gate opening motif boxed in red. The penultimate tyrosine is conserved in all proteins, with ORF68 having the most canonical "LYA" sequence. **(B)** Co-IP western blot of ORF68ΔLYA and ORF68-TS showing that deletion or masking of the gate opening motif does not disrupt the ORF68-proteasome interaction.

Deletion or masking of the ORF68 gate opening motif inhibits the degradation of a model substrate in transfected cells

To determine if the HbYX gate opening motif of ORF68 is functional, we measured its effect on the proteasome-mediated degradation of a model substrate in HEK293T cells. Destabilized GFP (dsGFP) was used as a model substrate, which was destabilized by the addition of a PEST domain derived from mouse ornithine decarboxylase (MODC). MODC targets proteins for proteasome-mediated degradation through an unknown mechanism but, importantly, it is independent of ubiquitin (Li et al., 1999). This means that changes in protein half-life can be attributed to the proteasome rather than upstream deubiquitinases. An additional benefit is that dsGFP has a short half-life in cells or approximately 4 hours (Glaunsinger and Ganem, 2004).

We first demonstrate that the degradation of dsGFP is proteasome-dependent under these conditions by measuring GFP half-life with and without the proteasome inhibitor MG132 by cycloheximide (CHX) treatment and western blot. The western blot signal of dsGFP is almost entirely absent by 4 hours post CHX treatment, whereas in cells treated with MG132 there is no

noticeable degradation even after 8 hours (Figure 4a). Next, we measured dsGFP half-life in the presence of ORF68, ORF68-TS, and ORF68ΔLYA. While ORF68 had no significant effect on dsGFP half-life, it was significantly extended by both ORF68-TS and ORF68ΔLYA. This can be seen both qualitatively by western blot (Figure 4b), and quantitatively by measuring the rate of dsGFP signal disappearance (Figure 4c). Interestingly, both ORF68-TS and ORF68ΔLYA were less stable than ORF68, evidenced by their gradual degradation during the time course (Figure 4b).

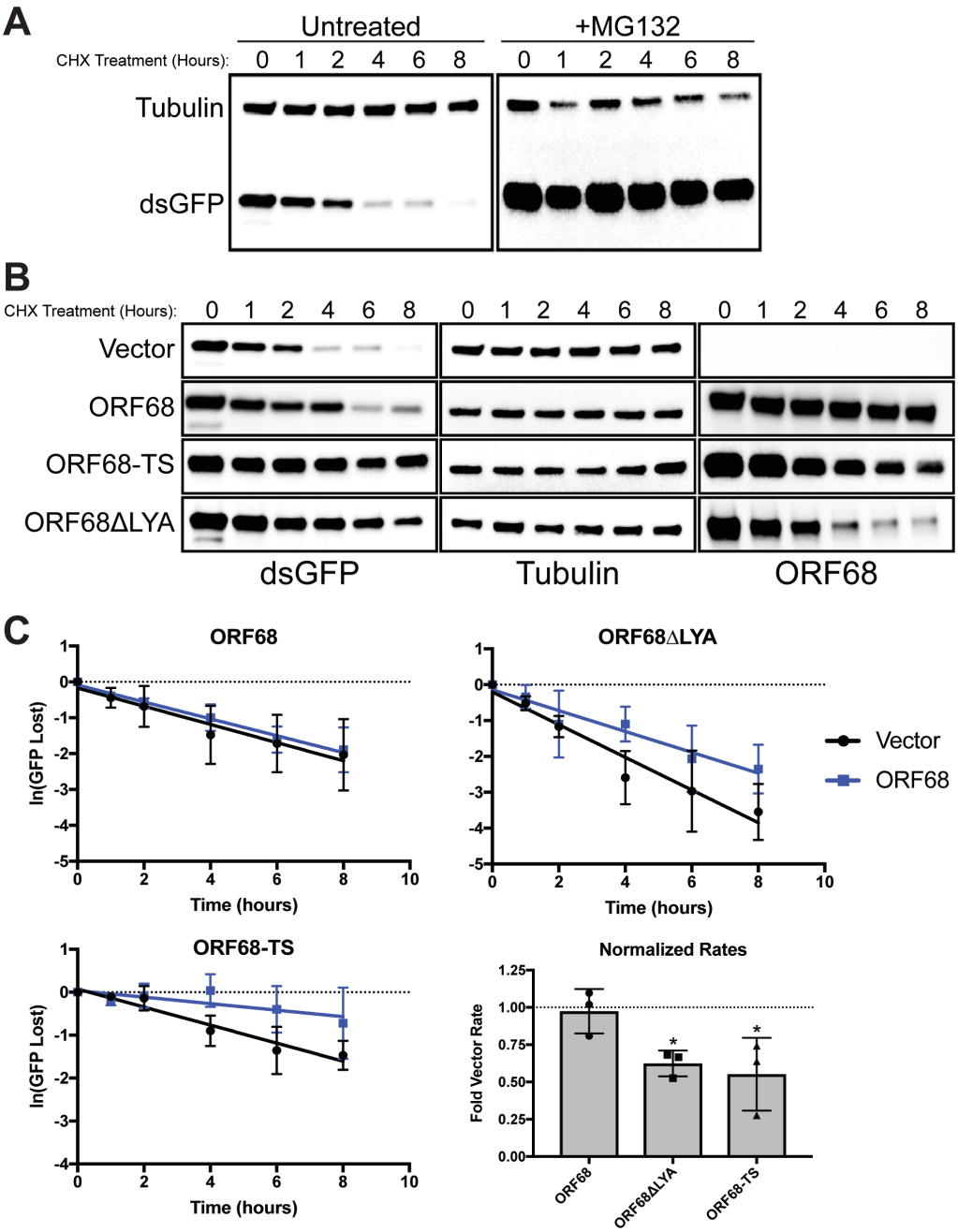

Figure 3.4. Deletion of the HbYX gate opening motif impairs the degradation of a model substrate in transfected cells. (A) Western blot showing that dsGFP is lost following cycloheximide (CHX) treatment. This effect is rescued by the proteasome inhibitor MG132. **(B)** Representative western blots of dsGFP half-life assays performed with the indicated ORF68 constructs. Tubulin serves as a loading control. **(C)** Quantification of GFP half-life assays shown in **(B)** with three biological replicates. ORF68 (blue squares) and Vector (black circles) slopes represent the natural log of dsGFP signal lost per hour, error bars represent standard deviation. The bar graph shows rate of rate of GFP loss normalized to paired vector controls, error bars represent standard deviation (* = $p < 0.05$).

The ORF68 gate opening motif is required for the production of infectious virions

We next wanted to determine if the gate opening motif in ORF68 is required for the KSHV replication cycle. Previous studies have shown that deletion of ORF68 results in a defect during cleavage and packaging of the viral genome (Gardner and Glaunsinger, 2018), so finer mutations were designed here. Using the BAC16 Red Recombinase system (Brulois et al., 2012), two mutants were made. The first deleted the LYA motif from ORF68 by replacing the codons for Leu and Tyr with Stop codons, called ORF68ΔLYA. The second appended a TwinStrep tag onto the carboxyl terminus of ORF68, thereby masking the gate opening motif, called ORF68-TS. The corresponding mutant rescue viruses were engineered from these mutants, ORF68ΔLYA-MR and ORF68-TS-MR, to ensure that no mutations outside of ORF68 had occurred during the mutagenesis process.

Both viruses were assayed for the production of infectious virions by supernatant transfer, where the filtered supernatant from reactivated cells is applied to uninfected target cells, which are then evaluated for the expression of GFP from the viral genome. In this assay, neither ORF68ΔLYA nor ORF68-TS produced infectious virions, whereas WT KSHV, ORF68ΔLYA-MR, and ORF68-TS-MR produced sufficient virus to infect nearly 100% of target cells (Figure 5a). ORF68ΔLYA and ORF68ΔLYA-MR were additionally assayed for viral gene expression using a variety of antibodies. These western blots showed that there was no defect in early gene expression, as evidenced by the ORF59 signal remaining unchanged between samples. However, late gene expression was slightly repressed.

A complication of interpreting any defects upon mutation or blocking of the LYA motif in the above KSHV mutants was that in both cases, expression of ORF68 itself was significantly reduced. To circumvent this problem, we sought to establish a complementation system in which equivalent levels of WT or altered ORF68 were expressed, thereby enabling us to distinguish phenotypes specifically linked to the LYA motif. Here, ORF68^{PTC} cells (Gardner and Glaunsinger, 2018) were complimented with WT ORF68 on an inducible cassette, which was stably integrated. The levels of ORF68 expressed by these cells was less than that of WT KSHV or even ORF68ΔLYA (Figure 5c). Despite this, complemented cells were able to produce virions sufficient to infect ~15% of target cells (Figure 5d). While this is much lower than WT levels of infection, it establishes that nearly any amount of WT ORF68 will allow for the production of virions, while even elevated levels of ORF68ΔLYA will not.

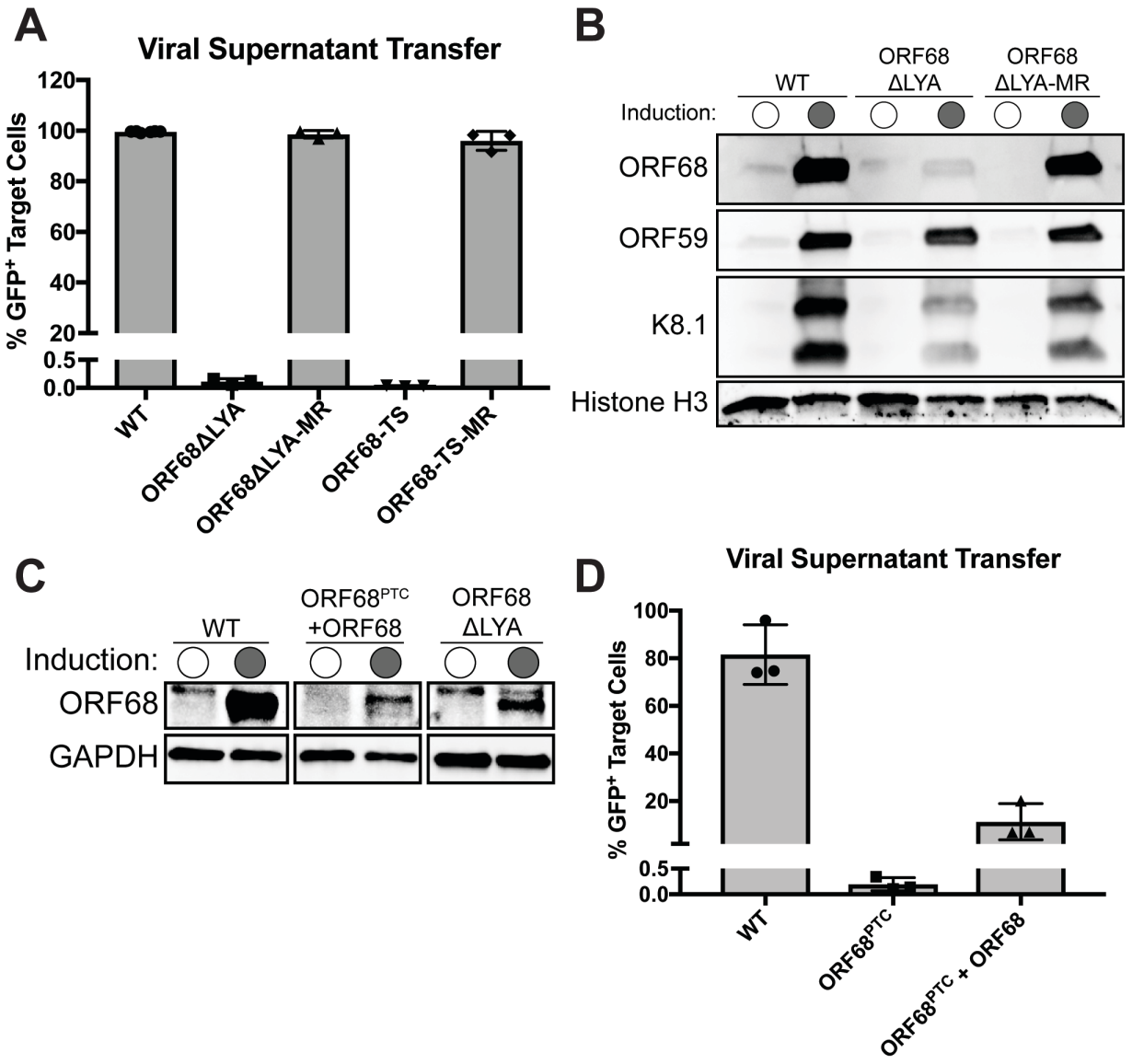

Figure 3.5. Characterization of the ORF68ΔLYA and ORF68-TS viruses. (A) Progeny virion production of ORF68 gate opening mutants was assayed by supernatant transfer and flow cytometry of target cells. **(B)** Western blots showing that deletion of the ORF68 gate opening motif reduces ORF68 stability, but did not after early gene expression (ORF59). Late gene expression (K8.1) is repressed. **(C)** Western blot of ORF68 expression in WT BAC16 (WT), ORF68^{PTC} BAC16 complimented with an inducible ORF68 gene (ORF68^{PTC} + ORF68), and ORF68ΔLYA BAC16. GAPDH serves as a loading control. **(D)** Progeny virion production of ORF68^{PTC} + ORF68 assayed by supernatant transfer.

Discussion

These data establish KSHV ORF68 as a proteasome-interacting protein whose gate opening motif is essential for virion production. This is the first description of a virally-encoded proteasome activator that suggests a novel mechanism for viral manipulation of the host proteasome. While many pathogens are known to interact with and manipulate the ubiquitin-proteasome system, these are almost universally at the ubiquitination stage. The few proteins which do directly act on the proteasome generally inhibit its assembly, as is the case of HIV-1 tat (Apcher et al., 2003; Seeger et al., 1997), or are difficult to degrade and obstruct proteolysis, as is the case of KSHV LANA (Zaldumbide et al., 2007). The proposed ability of KSHV ORF68 to control proteasome activity by encoding a gate opening protein may allow KSHV to more broadly control both host and viral protein levels during infection. In this regard, a key future goal will be to identify the native protein targets whose degradation is controlled by ORF68 during KSHV infection. Given the requirement for ORF68 in viral DNA packaging, one exciting possibility is that ORF68 directs the proteasome to remove replication or transcription complexes (or other DNA bound proteins) from the viral DNA to facilitate its threading into the nascent capsid.

The KSHV interactome shed light on numerous host-viral protein-protein interactions that were previously unappreciated (Davis et al., 2015b). The ORF68 interaction network is dominated by fourteen different subunits of the 26S proteasome, a strong indication that this is a relevant interaction. The interaction between ORF68 and the proteasome was confirmed by co-IP with tagged subunits of the 20S proteasome. This strategy was devised based on purification strategies employed in yeast and is both robust and specific, based on the fact that once assembled, the 20S cannot disassociate into its constituent subunits (Beckwith et al., 2013). ORF68 was seen to robustly co-purify with the 20S proteasome, while another viral protein, ORF59, did not. This is an important control because ORF59 was not predicted by the interactome to interact with the proteasome (Davis et al., 2015b), and is localized to the same viral replication compartments during infection (Gardner and Glaunsinger, 2018). These data demonstrate the specificity of the ORF68-proteasome interaction.

This interaction was also confirmed to occur during infection. Although the proteasome is dispersed throughout the cell during latency, it is concentrated in replication compartments during the lytic cycle. This closely matches the localization of ORF68 and, although they do not overlap perfectly, they colocalize much more in the nucleus than in the cytoplasm. Replication compartments are lobed structures in the nuclei of infected cells that do not stain well with DAPI and are the site of viral DNA replication and virion assembly. Given the wide array of processes that occur in replication compartments, it is unsurprising that there are so many proteasomes localized there. Proteasomes play a role in transcription, DNA replication, and protein quality control, all of which are undoubtedly vital in these very active sites during viral replication (Abbas and Dutta, 2018; Amm et al., 2014; Durairaj and Kaiser, 2014).

Given the interaction between ORF68 and the proteasome, we sought to find regions of ORF68 that are important for this interaction. With herpesviruses, it is useful to look at homologous proteins in related herpesviruses, as residues that are conserved over the millions of years of divergent evolution separating these viruses are often important for their function. The amino acid alignment of ORF68 and homologs showed less than 30% identity, but there are

several residues that are conserved throughout all human herpesviruses. One of these residues is a penultimate Tyrosine at the carboxyl-terminus of the proteins, which is part of a larger Hb-Y-X gate opening motif. This motif is an important proteasome-interaction motif that stands for Hydrophobic-Tyrosine-Any amino acid and must be at the very carboxyl-terminus of the protein in question (Bard et al., 2018). The gate opening motif of ORF68 best fits the motif definition as it has the sequence LYA, the leucine of which is much more hydrophobic than the amino acids at that position in the other homologs. However, the most important part of a gate opening motif if the penultimate tyrosine, which is absolutely required, whereas there are examples of gate opening motifs with less hydrophobic residues in the first position (la Peña and Lander, 2016). Furthermore, it has been observed that addition of a carboxyl-terminal tag to the HCMV homolog of ORF68 prevented the production of infectious virions, whereas an amino-terminal tag did not (Borst et al., 2008). This further argues that the HbYX motif is both conserved between the herpesviruses and that its activity required for the viral replication cycle.

Gate opening motifs are of particular interest because they are the mechanism through which native proteasome activators engage with the 20S core peptidase and allow for proteolysis. The 20S proteasome is a chambered peptidase with the proteolytic active sites sequestered in the lumen, to prevent rampant, uncontrolled protein degradation. The most well studied proteasome activator in eukaryotes is the 19S regulatory particle, which is part of the 26S holoenzyme and the end of the ubiquitin-proteasome pathway. However, unlike the 19S (Smith et al., 2007), deletion or masking of ORF68's gate opening motif does not ablate its interaction with the proteasome. This may hint at the nature of the ORF68-proteasome interaction, where ORF68 could displace the 19S regulatory particle to alter what proteins are degraded during infection.

To examine the possibility of ORF68 changing the degradation of substrates by the proteasome, we measured the effect of ORF68 expression on the degradation of a model substrate. This was accomplished by monitoring the degradation of a destabilized GFP (dsGFP) construct in cells that were treated with cycloheximide, thereby preventing the production of new proteins. Importantly, dsGFP was destabilized by the addition of the PEST domain from mouse ornithine decarboxylase, which targets fused proteins for proteasomal degradation in a ubiquitin-independent manner (Li et al., 1999). In bypassing the ubiquitination machinery, we assure that what we are measuring is proteasome-mediated proteolysis, instead of deubiquitination. In performing these assays, we observed that ORF68 did not significantly affect the rate of dsGFP degradation. Qualitatively, it appears that the dsGFP signal may be longer-lasting, but when the starting quantities are taken into consideration, the rate of dsGFP degradation is not different from cells transfected with the expression vector alone. However, by deleting the gate opening motif, in the case of ORF68ΔLYA, or masking it, in the case of ORF68-TS, dsGFP degradation is significantly inhibited. These data suggest that while the gate opening motif of ORF68 is intact, it does not impede the degradation of dsGFP. On the other hand, when the gate opening motif is not functional, we hypothesize that ORF68 acts as a dominant negative by continuing to bind to the proteasome while no longer being able to open the 20S gate. ORF68 may additionally prevent the binding of other proteasome activators, because dsGFP is well degraded in the absence of ORF68, whereas nonfunctional ORF68 prevents its degradation. Furthermore, ORF68-TS and especially ORF68ΔLYA are less stable than native ORF68. If the

mutant ORF68 proteins had a stability closer to that of native ORF68 it is likely that the proteasome inhibition would be even more pronounced.

By examining the importance of this motif in the context of the virus, we showed that deletion or masking of the gate opening motif completely prevented the production of progeny virions. Thus, we propose that ORF68 modulates substrate access to the 20S core in a manner that is vital to the replication cycle of KSHV. Furthermore, it is not just the localization of ORF68 to the proteasome that is important, because both of these mutants can still interact with the proteasome, as shown by co-IP. It is important to note that while there is a marked defect in the expression of these mutants compared to native ORF68, this cannot be the reason no virions are produced. Expression of very low levels of native ORF68 is enough to partially rescue virus lacking ORF68, while even higher levels of ORF68ΔLYA cannot complement the same virus. The instability of mutant ORF68 is not entirely surprising, as localization of proteins to the proteasome is often enough to increase their proteasome-mediated degradation. It is easy to envision how a protein that is localized directly adjacent to the 20S gate would be at risk for higher levels of degradation, especially when it is missing an important interaction motif. In a similar vein, it is interesting that the ORF68ΔLYA mutant has a slight defect in late gene expression, while the virus completely lacking ORF68 does not (Gardner and Glaunsinger, 2018). This may be caused by a dominant negative effect of ORF68ΔLYA, where it is more deleterious to have protein localized to the proteasome which cannot open the gate than it is to not have that protein at all. This again suggests that ORF68 can displace other proteasome activators, or at least prevent their binding to the 20S core once it is already bound. Confirmation and characterization of how ORF68 binds to the proteasome will require *in vitro* experimentation and most likely structure determination of ORF68. These represent significant challenges, given the difficulty of purifying sufficient amounts of ORF68 and mammalian proteasome of defined composition, but are nonetheless exciting future directions.

Methods

Plasmids

ORF68 and ORF59 with carboxyl-terminal TwinStrep tags were generated previously (Davis et al., 2015b), as was tagless ORF68 (Gardner and Glaunsinger, 2018). Production of destabilized GFP (dsGFP) was reported previously (Glaunsinger and Ganem, 2004). ORF68ΔLYA was produced with primers 5'-TGGAATTCTGCAGATATGTTTGTTCCCTGGCAACTCG-3' and 5'-GCCACTGTGCTGGATTCAGTGTGACGTCTGTGAGGGGT-3'. C-terminally tagged PSMB4-Strep was produced first with primers 5'-CTGCTACCGTGACTAAGATGGAAGC-3' and 5'-CAAAAGAAGAGTCTATCTTTGAACTAGCCAAGTTC-3' which annealed to cDNA derived from HFF-1 cells (ATCC SCRC-1041), and then with primers 5'-TACCGAGCTCGGATCATGGAAGCGTTTTTGGGGTCG-3' and 5'-CTCCCTCGAGCGGCCCTTCAAAGCCACTGATCATGTGGGC-3', which annealed to the first product. All PCR products were inserted into pCDNA4 (ThermoFisher) by InFusion cloning (Clontech). ORF68ΔLYA was inserted into the EcoRV site, and PSMB4-Strep into the BamHI and NotI sites. Inducible ORF68 complementation in BAC16 ORF68^{PTC} was accomplished by cloning ORF68 into the TetOne inducible vector (Clontech) which had the puromycin resistance replaced with zeocin

resistance. The ORF68 insert was generated using 5'-CCCTCGTAAAGAATTATGTTTGTTCCCTGGCAACTCG-3' and 5'-GAGGTGGTCTGGATCTTAGTGTGACGTCTGTGAGGGGTG-3' and inserted into the vector digested with EcoRI and BamHI.

Cell Lines

iSLK.BAC16 (Brulois et al., 2012) cells were maintained in DMEM + 10% FBS, 1 mg/ml hygromycin B, and 1 µg/ml puromycin. HEK293T (ATCC CRL-3216) cells were maintained in DMEM +10% FBS. HEK293T-ORF68 cells were maintained in DMEM + 10% FBS, 325 µg/ml zeocin. iSLK.BAC16 ORF68^{PTC} + ORF68 cells were generated using the above detailed pTetOne-Zeo-ORF68 plasmid according to the manufacturer's instructions. Briefly, the donor plasmid was mixed with Lenti-X Packaging Single Shots (VSV-G) mix, transfected into HEK293T cells, and the supernatant harvested after 48 hours. The supernatant was filtered, diluted 1:3 with fresh media and used to spinfect iSLK.BAC16 ORF68^{PTC} cells. Selection was accomplished with 1 mg/ml zeocin for 2 weeks.

Proteasome Immunoprecipitations

For co-immunoprecipitation experiments during overexpression, HEK293T cells were transfected with the indicated combinations of plasmids using linear polyethylenimine (PEI, MW ~25,000) at a 1:3 DNA:PEI ratio. Cells were harvested 24 hours after transfection in protein lysis buffer (50 mM Tris-HCl pH 7.6, 150 mM NaCl, 5 mM ATP, 3 mM $MgCl_2$, 1 mM DTT, 10% glycerol, 0.5% NP-40, cOmplete EDTA-free Protease Inhibitors [Roche]) and clarified by centrifugation at 20,000 x *g* for 10 min at 4˚C. Protein content in clarified supernatants was quantified by Bradford Assay (Bio-Rad) and 1 mg was applied to 20 µl of 3x washed MagStrep III beads (IBA). The total volume was brought to 1 ml using protein lysis buffer and the samples were rotated at 4˚C for 1 hour. The beads were washed 3x with 1 ml of IP wash buffer (50 mM Tris-HCl pH 7.6, 150 mM NaCl, 5 mM ATP, 3 mM $MgCl_2$, 1 mM DTT, 10% glycerol, 0.05% NP-40), using a magnet to retain the beads. Protein was eluted from the beads by resuspending in 2x Laemmli buffer and boiling for 10 minutes. The resulting eluate was resolved by SDS-PAGE and visualized by western blotting. For FLAG-IPs the same protocol was followed until elution, where instead of boiling the M2-FLAG beads (Sigma) were washed 3 times with IP wash buffer with no NP-40. Protein was then eluted in the same buffer with 150 µg/ml 3xFLAG peptide (Sigma), agitated for 30 minutes at 4˚C. Native proteasome purifications were performed in the same buffers and using the same protocol, but with RAD23-UBL agarose beads (Fisher Scientific). A magnet could not be used for these beads, so the they were pelleted at 1,000 x *g*, 4˚C and the supernatant removed for all wash steps.

ClustalOmega Alignment

Protein sequences for the indicated proteins were obtained from UniProt (https://www.uniprot.org/) and aligned using ClustalOmega (https://www.ebi.ac.uk/Tools/msa/clustalo/) using the default parameters.

Viral mutagenesis

The KSHV ORF68 gate opening motif deletion (ORF68ΔLYA) and C-terminal TwinStrep tag (ORF68-TS) mutant were engineered using the scarless Red recombination system in BAC16 GS1783 *E. coli* as previously described (Brulois et al., 2012). Modifications to the protocol and the establishment of infection by co-culture, as well as establishment of the ORF68^{PTC} BAC16 mutant, are detailed in (Gardner and Glaunsinger, 2018). Briefly, recombinant BAC16 is transfected into 293T cells, which are co-cultured 1:1 with uninfected iSLK cells. Virion production is induced from the 293T cells by the addition of 30 nM 12-O-Tetradecanoylphorbol-13-acetate (TPA) and 300 mM sodium butyrate, which over the course of four days infect the iSLK cells. Infected iSLK cells are then selected with a combination of hygromycin B (1 mg/ml), puromycin (1 µg/ml), and G418 (250 µg/ml). In the case of lethal mutations, as seen here, the 293T cells are first complimented with the wild type form of the protein. For ORF68, these cells were previously generated (Gardner and Glaunsinger, 2018) and were used to make these mutant viruses.

Mutant Virus Characterization

Cells latently infected with KSHV-BAC16 were induced into the lytic cycle by the addition of 1 µg/ml doxycycline and 1 mM sodium butyrate. Cells were reactivated for 48 hours for immunoprecipitation and western blot experiments and for 72 hours for supernatant transfer assays. Supernatant transfers were performed as previously described (Gardner and Glaunsinger, 2018). Briefly, the supernatant from reactivated cells is filtered and transferred onto uninfected 293T cells, which can then be assayed for the GFP expressed from the viral genome after 24 hours.

Western blots and antibodies

All western blots were performed on protein samples resolved by SDS-PAGE on 4 - 15 % polyacrylamide gels. Western blots were performed using rabbit anti-ORF68 (1:5000), rabbit anti-ORF59 (1:10,000), rabbit anti-K8.1 (1:10,000), rabbit anti-histone H3 (1:3000, Cell Signaling 4499S), mouse anti-Strep Tag II (1:3000, ThermoFisher SAB2702216), mouse anti-β tubulin (1:2500, Sigma T5293), mouse anti-GFP (1:5000, Clontech 632381), rabbit anti-RPN11 (1:5000, Abcam ab109130), rabbit anti-RPT6 (1:5000, Abcam ab178681), or mouse anti-PSMB7 (1:1000, Santa Cruz Biotech sc-398323). Rabbit anti-ORF68, -ORF59, and -K8.1 were produced in rabbits as previously described (Gardner and Glaunsinger, 2018).

Immunofluorescence assays

Cells were fixed with 4% paraformaldehyde in PBS for 10 minutes at room temperature, permeabilized with ice-cold methanol for 20 minutes at -20˚C, and blocked with BSA blocking buffer (PBS, 1% Triton X-100, 0.5% Tween20, 3% BSA) for 30 minutes at room temperature. The cells were then stained with rabbit anti-ORF68 and mouse anti-PSMB7 diluted 1:100 in BSA Blocking buffer overnight at 4˚C, washed three times with PBS, and incubated with secondary antibodies (AlexaFluor594 or DyLight650 [ThermoFisher], 1:1000 in BSA blocking buffer) for 1 h at 37˚C, before being mounted using VectaShield HardSet with DAPI (ThermoFisher). Images were acquired on an EVOS FL inverted fluorescent microscope (ThermoFisher).

GFP Half-life Assay

Twelve well plates seeded HEK293T cells were transfected with the indicated plasmids (700 ng), as well as dsEGFP (100 ng) using PEI as described above. Twenty-four hours post-transfection, cycloheximide (Sigma) was added (100 μg/ml) to stop further protein production. Wells were harvested after the indicated time by washing with PBS, resuspending in protein lysis buffer, and storing at -80˚C. Samples were then resolved by SDS-PAGE and western blotted for the indicated proteins. For cells treated with MG132 (Sigma), the drug was added to a final concentration of 30 μM concurrently with cycloheximide. Dosimetry of western blots was performed with ImageLab v6 (Bio-Rad), GFP signal was normalized to β-tubulin signal, to account for loading differences, before all lanes were normalized to T0 to account for differences in the starting GFP pool. The resulting values were analyzed with Prism v7 (GraphPad) by linear regression of the natural log, using least-squares fit.

Acknowledgements

We thank all past and members of the Glaunsinger, Coscoy, and Martin labs, in particular Zoe Davis, Apurva Govande, and Michal Olszewski for their helpful suggestions, guidance and support throughout the entirety of this study.

Chapter 4: Perspectives and Concluding Remarks

Here we present a characterization of the KSHV protein ORF68. First, the role of ORF68 during viral DNA packaging and cleavage was assessed, revealing ORF68 to be required for viral DNA cleavage and virion production. This we attribute to its newly described DNA-binding activity. We also discovered that ORF68 was associated with metal-dependent nuclease activity and would completely degrade DNA substrates in the presence of certain divalent metal cations. Next, expanding on data reported in the KSHV interactome, we examined ORF68's ability to bind to the host proteasome. ORF68 was confirmed to co-purify with the host proteasome from both transfected and infected cells by co-IP western blot. Furthermore, a proteasome-interacting motif in ORF68 and homologs in other herpesviruses suggested that ORF68 may act as a virally-encoded proteasome activator. While this motif was dispensable for proteasome interaction, deletion or masking of the motif significantly inhibited the degradation of a model substrate in cells. This activity was shown to be relevant to the virus as the same mutants in the context of infection prevented progeny virion production. Collectively, these data form the first description of KSHV ORF68 and establish it as a multifunctional viral protein whose disparate activities are both essential for the production of infectious virions.

Specificity of Nucleic Acid Binding by ORF68

The nucleic acid binding described for ORF68 utilized the subunit-length terminal repeat (TR) of KSHV, which was chosen because the TR is the site of DNA cleavage during viral DNA packaging. However, it is possible that ORF68 would bind any DNA probe given the correct conditions. This lack of specificity is actually suggested by the EMSA itself, as there are multiple shifts in mobility observed after the initial binding event. Given the large probe that was used, these most likely represent multiple ORF68 molecules binding each probe, which would in turn suggest that there is more than one place that ORF68 can bind. This may represent the repetitive nature of the TR itself, which could conceivably contain multiple, specific binding sites, but it is more likely that there is simply enough room for multiple proteins to bind. It would be fairly trivial to test specific probes for ORF68 binding, but it would be more informative to perform a screen of probes where the specific composition is altered slightly. The probes could then be assayed for which ORF68 binds the most readily. Determining the specificity of ORF68-nucleic acid binding would give valuable insight into the role it is playing during DNA packaging, as all that is confirmed here is that ORF68 binds to the TRs *in vitro* and that the genome is not cleaved in its absence.

Once the specificity of the interaction is known, it would be of great interest to dissect where exactly ORF68 would bind its preferred substrates. This would ideally be accomplished through simply DNA foot printing assays, but the initial substrate screen could also be designed to be high enough resolution to determine a binding site. Depending on ORF68's interaction with the terminase complex itself, these data could give insight as to where the packaging motifs are in the TRs of KSHV, which are currently unknown. In a similar vein, the function of the homologs of ORF68 in other herpesviruses is largely unexplored and it would be informative to examine if these proteins behave similarly *in vitro*. Given that the DNA packaging reaction is central to herpesvirus biology, it is unlikely to have diverged significantly between viruses. Now that the

purification conditions of ORF68 are defined, the homologs might be purified and examined in a similar way.

The Nuclease Activity of ORF68

Our studies have demonstrated that ORF68 is associated with nuclease activity *in vitro*. However, as mentioned previously, there is no apparent substrate-specificity for this activity. Cleavage assays with the TR do show a time-dependent resolution into discrete bands, but no further characterization has been performed. It is formally possible that a cellular nuclease is co-purifying with ORF68, even though other proteins are undetectable by colloidal Coomassie staining and by mass spectroscopy. However, it remains to be proven that ORF68 is responsible for the observed nuclease activity. This formal proof would most likely take the form of a crystal structure, where the active site could be visualized and then mutagenized. A DNA-binding or nuclease defective ORF68 would be very informative to study both *in vitro* and during infection.

If ORF68 is a bona fide nuclease, the current observations of its activity raise a few obvious questions. First, why does ORF68 have no substrate-specificity *in vitro*? This is a question that has also been asked for the SOX nuclease, which can degrade RNAs *in vitro* that are not substrates in the cell (Covarrubias et al., 2011). ORF68 may behave in a similar way, which could be assessed by developing an *in vivo* cleavage assay. If true, the next step would be to ask what confers said specificity and an approach similar to what has been done for KSHV SOX could be employed. Second, why does ORF68 cleave DNA so slowly? This question if largely borne of the fact that overnight digestions were required to completely degrade the TR substrate, whereas DNase I degrades the same substrate in minutes. This may reflect that the substrate is lacking a true ORF68 cleavage site and what we observe is simply non-specific activity at a much lower rate. Alternatively, it could be that ORF68 requires a cofactor missing from the *in vitro* assays, which could be another protein or ion. It may also be that ORF68 does not need to be a fast enzyme, as the viral genome is processively threaded into a nascent capsid and the geometry of this process could allow ORF68 to cut much more efficiently as the genome is forced passed it. Lastly, given that ORF68 is always observed as an oligomer in solution, is this oligomerization relevant for DNA binding and cleavage? The oligomeric state of ORF68 is an alternative explanation for the cooperativity observed by EMSA and may be relevant for the role that ORF68 plays in processing the viral genome. To evaluate the contribution of oligomerization, ORF68 mutants that cannot oligomerize would have to be generated. Here, a crystal structure of ORF68 would help greatly, as it would not only define the oligomeric state, but reveal oligomerization domains. Depending on the true oligomeric state of ORF68 bound to DNA, the reported affinity could be an underestimate, and may be as low as 10 nM, which would put it on the same order of magnitude as the other terminase proteins that bind the terminal repeat (Adelman et al., 2001).

How does ORF68 interact with the Proteasome?

We show here that ORF68 co-purifies with the proteasome in a variety of conditions. However, the proteasome is a large, modular complex with many different subcomplexes. Defining the nature of the ORF68-proteasome interaction would be the next logical step and one that could further illuminate how ORF68 might manipulate substrate degradation. It is currently unclear if other proteins are required for ORF68 to interact with the proteasome, but if ORF68 is

a mimic of cellular proteasome activators, then it likely required accessory proteins for its activity. These could take the form of cellular proteins already known to associate with the proteasome, other viral proteins, or both, forming a chimeric complex. In any case, if ORF68 is proven to be a true proteasome activator then this would be the first report of a virus manipulating the proteasome in this way. As of now, the proteasome is often targeted by pathogens, but it is almost universally at the stage of ubiquitination or, in one case, assembly (Seeger et al., 1997). Co-opting the 20S core by displacing native proteasome activators would be an elegant and efficient way to control the host proteome, but would be a complex endeavor and has yet to be proven to occur.

The two experiments that would prove this hypothesis most succinctly would be a co-structure of ORF68 and the 20S proteasome, ideally by cryo-electron microscopy, and an identification of substrates degraded by this alternative proteasome. Negative stain and cryo-electron microscopy have been used very successfully with the proteasome in the past and there is no reason to believe they would not be successful with ORF68. These experiments would ideally occur as an *in vitro* reconstitution, but if ORF68 requires accessory proteins to efficiently interact with the proteasome, then the established co-IP purifications could be used. Identification of substrates specific to this putative complex will likely require whole cell proteomics. This would most likely take the form of tandem mass tags (TMT) or direct spectral counting, depending on the available mass spectrometry equipment. Ideally, cells infected with WT KSHV would be compared to KSHV mutant viruses lacking ORF68 or with ORF68ΔLYA, which would show which proteins are more or less abundant when ORF68 commandeers the proteasome.

Other Proteasome-Interacting Proteins in KSHV

These data focus of the strongest viral protein-proteasome interaction identified by the KSHV interactome, but it is not the only association that was discovered. KSHV ORF23, ORF24, ORF29, ORF62, and ORF66 were all found to purify with multiple subunits of the proteasome, although with lower confidence than their other interactions (Davis et al., 2015b). Of these, ORF24, ORF29, and ORF66 are of particular interest. ORF29 is a part of the terminase enzyme which actually threads the replicated genomes into nascent capsids during the DNA packaging process and has additionally been shown to have an RNase H – like fold that can nick DNA substrates *in vitro* (Selvarajan Sigamani et al., 2013). If relevant, this interaction could confirm that the proteasome has a role to play in viral DNA packaging and is not a disparate activity of ORF68. ORF24 and ORF66 are both members of the viral late gene pre-initiation complex, which are required for the expression of a class of genes during gammaherpesvirus infection (Davis et al., 2015a). Considering that the proteasome itself is required for efficient transcription (Durairaj and Kaiser, 2014), could this interaction be relevant for the expression of late genes? Similar co-IP western blot experiments to those performed with ORF68 would confirm the interactions, which could be then be perturbed and evaluated during viral infection. Another exciting possibility is the interaction of all of these viral proteins to form the putative “viral proteasome activator” that has been postulated here.

Are the Activities of ORF68 Related?

There are countless examples of viral proteins that play more than one role in the cell during infection. Given the data presented here, it is interesting to hypothesize that the proteasome-manipulation and DNA-processing activities of ORF68 are in some way related. For instance, it has been shown that the viral DNA in mature capsids is packed nearly to the theoretical limit of non-crystalline substances and could therefore not contain any protein or accessory nucleic acids (McElwee et al., 2018). ORF68 could then be responsible for trimming DNA branches or hybridized RNA from the genome during packaging, by means of its DNA-binding and nuclease activity, while simultaneously removing bound proteins by recruiting and activating the 20S proteasome. This would explain why deletion of the gate opening motif would also prevent the production of virions, in the same way as deletion of the entire ORF would. However, immunofluorescence assays of ORF68 during infection also show localization to distinct puncta in the cytoplasm, as well as large, perinuclear aggregates. The later of these additionally shows proteasome co-localization, so it may be that ORF68's proteasome interaction has an additional, cytoplasmic function completely separate from nuclear DNA packaging. Investigation of the two activities would require genetically separable domains, but given that the gate opening motif must be located at the carboxyl-terminus this should be possible. A structure would once again enable elegant, targeted mutations, but it would also be possible to mutagenize each of the conserved residues in ORF68 individually and assay them for loss of one function or the other. In the end, it could be that both possibilities are true. Nuclear ORF68 may manipulate nuclear proteasomes in addition to binding and processing the viral genome during packaging, while at the same time manipulating cytoplasmic proteasomes, which often play very different roles than their nuclear counterparts.

Chapter 5: References

Abbas, T., and Dutta, A. (2018). Regulation of Mammalian DNA Replication via the Ubiquitin-Proteasome System. In Human Herpesviruses, (Singapore: Springer Singapore), pp. 421–454.

Abernathy, E., Clyde, K., Yeasmin, R., Krug, L.T., Burlingame, A., Coscoy, L., and Glaunsinger, B. (2014). Gammaherpesviral Gene Expression and Virion Composition Are Broadly Controlled by Accelerated mRNA Degradation. PLoS Pathog *10*, e1003882–14.

Abernathy, E., Gilbertson, S., Alla, R., and Glaunsinger, B. (2015). Viral Nucleases Induce an mRNA Degradation- Transcription Feedback Loop in Mammalian Cells. Cell Host and Microbe *18*, 243–253.

Adams, J. (2004). The Proteasome in Cell-Cycle Regulation (Totowa, NJ: Humana Press).

Adelman, K., Salmon, B., and Baines, J.D. (2001). Herpes simplex virus DNA packaging sequences adopt novel structures that are specifically recognized by a component of the cleavage and packaging machinery. Proc Natl Acad Sci USA *98*, 3086–3091.

Albright, B.S., Kosinski, A., Szczepaniak, R., Cook, E.A., Stow, N.D., Conway, J.F., and Weller, S.K. (2014). The Putative Herpes Simplex Virus 1 Chaperone Protein UL32 Modulates Disulfide Bond Formation during Infection. *89*, 443–453.

Amm, I., Sommer, T., and Wolf, D.H. (2014). Protein quality control and elimination of protein waste: The role of the ubiquitin–proteasome system. BBA - Molecular Cell Research *1843*, 182–196.

Apcher, G.S., Heink, S., Zantopf, D., Kloetzel, P.M., Schmid, H.-P., Mayer, R.J., and Krüger, E. (2003). Human immunodeficiency virus-1 Tat protein interacts with distinct proteasomal α and β subunits. FEBS Letters *553*, 200–204.

Arslan, P., Di Virgilio, F., Beltrame, M., Biological, R.T.J.O., 1985 (1985). Cytosolic Ca2+ homeostasis in Ehrlich and Yoshida carcinomas. A new, membrane-permeant chelator of heavy metals reveals that these ascites tumor cell lines have …. Asbmb. *260*, 2719–2727.

Ashizawa, A., Higashi, C., Masuda, K., Ohga, R., Taira, T., and Fujimuro, M. (2012). The Ubiquitin System and Kaposi's Sarcoma-Associated Herpesvirus. Front. Microbiol. *3*, 66.

Azab, W., and Osterrieder, K. (2017). Initial Contact: The First Steps in Herpesvirus Entry. In Cell Biology of Herpes Viruses, K. Osterrieder, ed. (Cham: Springer International Publishing), pp. 1–27.

Bagnéris, C., Briggs, L.C., Savva, R., Ebrahimi, B., and Barrett, T.E. (2011). Crystal structure of a KSHV–SOX–DNA complex: insights into the molecular mechanisms underlying DNase activity and host shutoff. Nucleic Acids Res *39*, 5744–5756.

Bard, J.A.M., Goodall, E.A., Greene, E.R., Jonsson, E., Dong, K.C., and Martin, A. (2018). Structure and Function of the 26S Proteasome. Annu. Rev. Biochem. *87*, 697–724.

Beckwith, R., Estrin, E., Worden, E.J., and Martin, A. (2013). Reconstitution of the 26S proteasome reveals functional asymmetries in its AAA+ unfoldase. Nature Structural &Amp; Molecular Biology *20*, 1164–1172.

Beltran, P.M.J., and Cristea, I.M. (2014). The life cycle and pathogenesis of human cytomegalovirus infection: lessons from proteomics. Expert Review of Proteomics *11*, 000–000.

Booy, F.P., Newcomb, W.W., Trus, B.L., Brown, J.C., Baker, T.S., and Steven, A.C. (1991). Liquid-crystalline, phage-like packing of encapsidated DNA in herpes simplex virus. Cell *64*, 1007–1015.

Borst, E.M., Wagner, K., Binz, A., Sodeik, B., and Messerle, M. (2008). The Essential Human Cytomegalovirus Gene UL52 Is Required for Cleavage-Packaging of the Viral Genome. J. Virol. *82*, 2065–2078.

Brulois, K.F., Chang, H., Lee, A.S.-Y., Ensser, A., Wong, L.-Y., Toth, Z., Lee, S.H., Lee, H.-R., Myoung, J., Ganem, D., et al. (2012). Construction and Manipulation of a New Kaposi's Sarcoma-Associated Herpesvirus Bacterial Artificial Chromosome Clone. J. Virol. *86*, 9708–9720.

Budenholzer, L., Cheng, C.L., Li, Y., and Hochstrasser, M. (2017). Proteasome Structure and Assembly. Journal of Molecular Biology *429*, 3500–3524.

Cardone, G., Winkler, D.C., Trus, B.L., Cheng, N., Heuser, J.E., Newcomb, W.W., Brown, J.C., and Steven, A.C. (2007a). Visualization of the herpes simplex virus portal in situ by cryo-electron tomography. Virology *361*, 426–434.

Cardone, G., Winkler, D.C., Trus, B.L., Cheng, N., Heuser, J.E., Newcomb, W.W., Brown, J.C., and Steven, A.C. (2007b). Virology *361*, 426–434.

Chang, P.-C., Campbell, M., and Robertson, E.S. (2016). Human Oncogenic Herpesvirus and Post-translational Modifications – Phosphorylation and SUMOylation. Front. Microbiol. *7*, 2388–5.

Chang, Y.E., Poon, A.P., and Roizman, B. (1996). Properties of the protein encoded by the UL32 open reading frame of herpes simplex virus 1. J. Virol. *70*, 3938–3946.

Chen, Z.J. (2005). Ubiquitin signalling in the NF-κB pathway. Nature Cell Biology *7*, 758–765.

Coscoy, L. (2007). Immune evasion by Kaposi's sarcoma-associated herpesvirus. Nat Rev Immunol *7*, 391–401.

Covarrubias, S., Gaglia, M.M., Kumar, G.R., Wong, W., Jackson, A.O., and Glaunsinger, B.A. (2011). Coordinated Destruction of Cellular Messages in Translation Complexes by the Gammaherpesvirus Host Shutoff Factor and the Mammalian Exonuclease Xrn1. PLoS Pathog *7*, e1002339–15.

Dai, X., Gong, D., Wu, T.T., Sun, R., and Zhou, Z.H. (2014). Organization of Capsid-Associated Tegument Components in Kaposi's Sarcoma-Associated Herpesvirus. J. Virol. *88*, 12694–12702.

Davis, Z.H., Hesser, C.R., Park, J., and Glaunsinger, B.A. (2015a). Interaction between ORF24 and ORF34 in the Kaposi's Sarcoma-Associated Herpesvirus Late Gene Transcription Factor Complex Is Essential for Viral Late Gene Expression. J. Virol. *90*, 599–604.

Davis, Z.H., Verschueren, E., Jang, G.M., Kleffman, K., Johnson, J.R., Park, J., Dollen, Von, J., Maher, M.C., Johnson, T., Newton, W., et al. (2015b). Global Mapping of Herpesvirus-Host Protein Complexes Reveals a Transcription Strategy for Late Genes. Molecular Cell *57*, 349–360.

Davison, A.J., Eberle, R., Ehlers, B., Hayward, G.S., McGeoch, D.J., Minson, A.C., Pellett, P.E., Roizman, B., Studdert, M.J., and Thiry, E. (2008). The order Herpesvirales. Arch Virol *154*, 171–177.

Deng, B., O'Connor, C.M., Kedes, D.H., and Zhou, Z.H. (2008). Cryo-electron tomography of Kaposi's sarcoma-associated herpesvirus capsids reveals dynamic scaffolding structures essential to capsid assembly and maturation. Journal of Structural Biology *161*, 419–427.

Dittmer, D.P., and Damania, B. (2016). Kaposi sarcoma–associated herpesvirus: immunobiology, oncogenesis, and therapy. Journal of Clinical Investigation *126*, 3165–3175.

Durairaj, G., and Kaiser, P. (2014). The 26S Proteasome and Initiation of Gene Transcription. Biomolecules *4*, 827–847.

Dyballa, N., and Metzger, S. (2009). Fast and Sensitive Colloidal Coomassie G-250 Staining for Proteins in Polyacrylamide Gels. JoVE 1–5.

Erales, J., and Coffino, P. (2014). Ubiquitin-independent proteasomal degradation. BBA - Molecular Cell Research *1843*, 216–221.

Ganem, D. (2006). KSHV infection and the pathogenesis of Kaposi's sarcoma. Annu Rev Pathol *1*, 273–296.

Gardner, M.R., and Glaunsinger, B.A. (2018). Kaposi's sarcoma-associated herpesvirus ORF68 is a DNA binding protein required for viral genome cleavage and packaging. J. Virol. JVI.00840–18–38.

Gibson, W., virology, B.R.J.O., (1972). Proteins specified by herpes simplex virus VIII. Characterization and composition of multiple capsid forms of subtypes 1 and 2. Am Soc Microbiol.

Glaunsinger, B., and Ganem, D. (2004). Lytic KSHV infection inhibits host gene expression by accelerating global mRNA turnover. Molecular Cell *13*, 713–723.

Golovine, K., Uzzo, R.G., Makhov, P., Crispen, P.L., Kunkle, D., and Kolenko, V.M. (2008). Depletion of intracellular zinc increases expression of tumorigenic cytokines VEGF, IL-6 and IL-8 in prostate cancer cells via NF-κB-dependent pathway. Prostate *68*, 1443–1449.

Goodrum, F. (2016). Human Cytomegalovirus Latency: Approaching the Gordian Knot. Annu. Rev. Virol. *3*, 333–357.

Grinde, B. (2013). Herpesviruses: latency and reactivation – viral strategies and host response. Journal of Oral Microbiology *5*, 22766–22769.

Gruffat, H., Marchione, R., and Manet, E. (2016). Herpesvirus Late Gene Expression: A Viral-Specific Pre-initiation Complex Is Key. Front. Microbiol. *7*, 13460–15.

Habison, A.C., de Miranda, M.P., Beauchemin, C., Tan, M., Cerqueira, S.A., Correia, B., Ponnusamy, R., Usherwood, E.J., McVey, C.E., Simas, J.P., et al. (2017). Cross-species conservation of episome maintenance provides a basis for in vivo investigation of Kaposi's sarcoma herpesvirus LANA. PLoS Pathog *13*, e1006555–25.

Hellert, J., Weidner-Glunde, M., Krausze, J., Lünsdorf, H., Ritter, C., Schulz, T.F., and Lührs, T. (2015). The 3D structure of Kaposi sarcoma herpesvirus LANA C-terminal domain bound to DNA. Proc Natl Acad Sci USA *112*, 6694–6699.

Heming, J.D., Conway, J.F., and Homa, F.L. (2017). Herpesvirus Capsid Assembly and DNA Packaging. In Cell Biology of Herpes Viruses, (Cham: Springer International Publishing), pp. 119–142.

Heming, J.D., Huffman, J.B., Jones, L.M., and Homa, F.L. (2014). Isolation and characterization of the herpes simplex virus 1 terminase complex. J. Virol. *88*, 225–236.

Hesser, C.R., Karijolich, J., Dominissini, D., He, C., and Glaunsinger, B.A. (2018). N6-methyladenosine modification and the YTHDF2 reader protein play cell type specific roles in lytic viral gene expression during Kaposi's sarcoma-associated herpesvirus infection. PLoS Pathog *14*, e1006995–23.

Hicke, L. (2001). Protein regulation by monoubiquitin. Nat Rev Mol Cell Biol *2*, 195–201.

Hyun, H.J., Sohn, J.H., Ha, D.W., Ahn, Y.H., Koh, J.Y., and Yoon, Y.H. (2001). Depletion of intracellular zinc and copper with TPEN results in apoptosis of cultured human retinal pigment epithelial cells. Invest. Ophthalmol. Vis. Sci. *42*, 460–465.

Izumiya, Y., Kobayashi, K., Kim, K.Y., Pochampalli, M., Izumiya, C., Shevchenko, B., Wang, D.-H., Huerta, S.B., Martinez, A., Campbell, M., et al. (2013). Kaposi's Sarcoma-Associated Herpesvirus K-Rta Exhibits SUMO-Targeting Ubiquitin Ligase (STUbL) Like Activity and Is Essential for Viral Reactivation. PLoS Pathog *9*, e1003506–e1003515.

Juillard, F., Tan, M., Li, S., and Kaye, K.M. (2016). Kaposi's Sarcoma Herpesvirus Genome Persistence. Front. Microbiol. *7*, 1883–1815.

Kish-Trier, E., and Hill, C.P. (2013). Structural Biology of the Proteasome. Annu. Rev. Biophys. *42*, 29–49.

Kuang, E., Fu, B., Liang, Q., Myoung, J., and Zhu, F. (2011). Phosphorylation of Eukaryotic Translation Initiation Factor 4B (EIF4B) by Open Reading Frame 45/p90 Ribosomal S6 Kinase (ORF45/RSK) Signaling Axis Facilitates Protein Translation during Kaposi Sarcoma-associated Herpesvirus (KSHV) Lytic Replication. J. Biol. Chem. *286*, 41171–41182.

Kwun, H.J., da Silva, S.R., Qin, H., Ferris, R.L., Tan, R., Chang, Y., and Moore, P.S. (2011). The central repeat domain 1 of Kaposi's sarcoma-associated herpesvirus (KSHV) latency associated-nuclear antigen 1 (LANA1) prevents cis MHC class I peptide presentation. Virology *412*, 357–365.

la Peña, de, A.H., and Lander, G.C. (2016). What"s the Key to Unlocking the Proteasome"s Gate? Structure/Folding and Design *24*, 2037–2038.

Labo, N., Miley, W., Marshall, V., Gillette, W., Esposito, D., Bess, M., Turano, A., Uldrick, T., Polizzotto, M.N., Wyvill, K.M., et al. (2014). Heterogeneity and Breadth of Host Antibody Response to KSHV Infection Demonstrated by Systematic Analysis of the KSHV Proteome. PLoS Pathog *10*, e1004046–11.

Li, D., Fu, W., and Swaminathan, S. (2018). Continuous DNA replication is required for late gene transcription and maintenance of replication compartments in gammaherpesviruses. PLoS Pathog *14*, e1007070–25.

Li, X., Zhao, X., Fang, Y., Jiang, X., Duong, T., Biological, C.F.J.O., 1998 (1999). Generation of destabilized green fluorescent protein as a transcription reporter. Asbmb *302*, 438–444.

Lorenzo, M.E., Jung, J.U., and Ploegh, H.L. (2002). Kaposi's Sarcoma-Associated Herpesvirus K3 Utilizes the Ubiquitin-Proteasome System in Routing Class I Major Histocompatibility Complexes to Late Endocytic Compartments. J. Virol. *76*, 5522–5531.

McElwee, M., Vijayakrishnan, S., Rixon, F., and Bhella, D. (2018). Structure of the herpes-simplex virus portal-vertex. 1–21.

Mettenleiter, T.C. (2002). Herpesvirus Assembly and Egress. J. Virol. *76*, 1537–1547.

Minor, M., and Slagle, B. (2014). Hepatitis B Virus HBx Protein Interactions with the Ubiquitin Proteasome System. Viruses *6*, 4683–4702.

Myoung, J., and Ganem, D. (2011). Generation of a doxycycline-inducible KSHV producer cell line of endothelial origin: Maintenance of tight latency with efficient reactivation upon induction. Journal of Virological Methods *174*, 12–21.

Nadal, M., Mas, P.J., Blanco, A.G., Arnan, C., Sola, M., Hart, D.J., and Coll, M. (2010). Structure and inhibition of herpesvirus DNA packaging terminase nuclease domain. Proc Natl Acad Sci USA *107*, 17059–17059.

Nakamura, H., Lu, M., Gwack, Y., Souvlis, J., Zeichner, S.L., and Jung, J.U. (2003). Global Changes in Kaposi's Sarcoma-Associated Virus Gene Expression Patterns following Expression of a Tetracycline-Inducible Rta Transactivator. J. Virol. *77*, 4205–4220.

Naranatt, P.P., Krishnan, H.H., Svojanovsky, S.R., Bloomer, C., Mathur, S., and Chandran, B. (2004). Host Gene Induction and Transcriptional Reprogramming in Kaposi's Sarcoma-Associated Herpesvirus (KSHV/HHV-8)-Infected Endothelial, Fibroblast, and B Cells. Cancer Research *64*, 72–84.

Newcomb, W.W., Homa, F.L., and Brown, J.C. (2006). Herpes Simplex Virus Capsid Structure: DNA Packaging Protein UL25 Is Located on the External Surface of the Capsid near the Vertices. J. Virol. *80*, 6286–6294.

Pavlova, S., Feederle, R., Gärtner, K., Fuchs, W., Granzow, H., and Delecluse, H.-J. (2013). An Epstein-Barr virus mutant produces immunogenic defective particles devoid of viral DNA. J. Virol. *87*, 2011–2022.

Pick, E., and Berman, T.S. (2013). Formation of alternative proteasomes: Same lady, different cap? FEBS Letters *587*, 389–393.

Piedade, D., and Azevedo-Pereira, J. (2016). The Role of microRNAs in the Pathogenesis of Herpesvirus Infection. Viruses *8*, 156–32.

Platteel, A.C.M., Liepe, J., Textoris-Taube, K., Keller, C., Henklein, P., Schalkwijk, H.H., Cardoso, R., Kloetzel, P.M., Mishto, M., and Sijts, A.J.A.M. (2017). Multi-level Strategy for Identifying Proteasome-Catalyzed Spliced Epitopes Targeted by CD8+ T Cells during Bacterial Infection. CellReports *20*, 1242–1253.

Renner, D.W., and Szpara, M.L. (2017). Impacts of Genome-Wide Analyses on Our Understanding of Human Herpesvirus Diversity and Evolution. J. Virol. *92*, e00908–17–13.

Rixon, F.J., and McNab, D. (1999). Packaging-competent capsids of a herpes simplex virus temperature-sensitive mutant have properties similar to those of in vitro-assembled procapsids. J. Virol. *73*, 5714–5721.

Rixon, F.J., Cross, A.M., Addison, C., and Preston, V.G. (1988). The products of herpes simplex virus type 1 gene UL26 which are involved in DNA packaging are strongly associated with empty but not with full capsids. Journal of General Virology *69 (Pt 11)*, 2879–2891.

Saji, C., Higashi, C., Niinaka, Y., Yamada, K., Noguchi, K., and Fujimuro, M. (2011). Proteasome inhibitors induce apoptosis and reduce viral replication in primary effusion lymphoma cells. Biochemical and Biophysical Research Communications *415*, 573–578.

Sancak, Y., Peterson, T.R., Shaul, Y.D., Lindquist, R.A., Thoreen, C.C., Bar-Peled, L., and Sabatini, D.M. (2008). The Rag GTPases Bind Raptor and Mediate Amino Acid Signaling to mTORC1. Science *320*, 1496–1501.

Seeger, M., Ferrell, K., Frank, R., and Dubiel, W. (1997). HIV-1 tat inhibits the 20 S proteasome and its 11 S regulator-mediated activation. J. Biol. Chem. *272*, 8145–8148.

Selvarajan Sigamani, S., Zhao, H., Kamau, Y.N., Baines, J.D., and Tang, L. (2013). The Structure of the Herpes Simplex Virus DNA-Packaging Terminase pUL15 Nuclease Domain Suggests an Evolutionary Lineage among Eukaryotic and Prokaryotic Viruses. J. Virol. *87*, 7140–7148.

Siggers, T., and Gordan, R. (2014). Protein-DNA binding: complexities and multi-protein codes. Nucleic Acids Res *42*, 2099–2111.

Smith, D.M., Chang, S.-C., Park, S., Finley, D., Cheng, Y., and Goldberg, A.L. (2007). Docking of the Proteasomal ATPases" Carboxyl Termini in the 20S Proteasome"s α Ring Opens the Gate for Substrate Entry. Molecular Cell *27*, 731–744.

Smith, G.A. (2017). Assembly and Egress of an Alphaherpesvirus Clockwork. In Cell Biology of Herpes Viruses, (Cham: Springer International Publishing), pp. 171–193.

Stadtmueller, B.M., and Hill, C.P. (2011). Proteasome Activators. Molecular Cell *41*, 8–19.

Straus, S.E., Cohen, J.I., Tosato, G., and Meier, J. (1993). Epstein-Barr virus infections: biology, pathogenesis, and management. Ann. Intern. Med. *118*, 45–58.

Tandon, R., Mocarski, E., and Conway, J. (2015). The A, B, Cs of Herpesvirus Capsids. Viruses *7*, 899–914.

Thurlow, J.K., Murphy, M., Stow, N.D., and Preston, V.G. (2006). Herpes Simplex Virus Type 1 DNA-Packaging Protein UL17 Is Required for Efficient Binding of UL25 to Capsids. J. Virol. *80*, 2118–2126.

Tong, L., and Stow, N.D. (2009). Analysis of Herpes Simplex Virus Type 1 DNA Packaging Signal Mutations in the Context of the Viral Genome. J. Virol. *84*, 321–329.

Ueda, K. (2018). KSHV Genome Replication and Maintenance in Latency. In Human Herpesviruses, (Singapore: Springer Singapore), pp. 299–320.

Varmuza, S.L., and Smiley, J.R. (1985). Signals for site-specific cleavage of HSV DNA: maturation involves two separate cleavage events at sites distal to the recognition sequences. Cell *41*, 793–802.

Vega Thurber, R.L., Barott, K.L., Hall, D., Liu, H., Rodriguez-Mueller, B., Desnues, C., Edwards, R.A., Haynes, M., Angly, F.E., Wegley, L., et al. (2008). Metagenomic analysis indicates that stressors induce production of herpes-like viruses in the coral Porites compressa. Proc. Natl. Acad. Sci. U.S.a. *105*, 18413–18418.

Wang, F., Durfee, L.A., and Huibregtse, J.M. (2013). A Cotranslational Ubiquitination Pathway for Quality Control of Misfolded Proteins. Molecular Cell *50*, 368–378.

Worden, E.J., Dong, K.C., and Martin, A. (2017). An AAA Motor-Driven Mechanical Switch in Rpn11 Controls Deubiquitination at the 26S Proteasome. Molecular Cell 1–22.

Wu, F.Y., Ahn, J.H., Alcendor, D.J., Jang, W.J., Xiao, J., Hayward, S.D., and Hayward, G.S. (2001). Origin-Independent Assembly of Kaposi's Sarcoma-Associated Herpesvirus DNA Replication Compartments in Transient Cotransfection Assays and Association with the ORF-K8 Protein and Cellular PML. J. Virol. *75*, 1487–1506.

Yang, W. (2010). Nucleases: diversity of structure, function and mechanism. Quart. Rev. Biophys. *44*, 1–93.

Yedidi, R.S., Wendler, P., and Enenkel, C. (2017). AAA-ATPases in Protein Degradation. Front. Mol. Biosci. *4*, 257–14.

Yu, D.E.A. (1998). Genetic Analysis of the UL15 Gene Locus for the Putative Terminase of Herpes Simplex Virus Type 1. 1–13.

Yu, Y., Wang, S.E., and Hayward, G.S. (2005). The KSHV Immediate-Early Transcription Factor RTA Encodes Ubiquitin E3 Ligase Activity that Targets IRF7 for Proteosome-Mediated Degradation. Immunity *22*, 59–70.

Zaldumbide, A., Ossevoort, M., Wiertz, E.J.H.J., and Hoeben, R.C. (2007). In cis inhibition of antigen processing by the latency-associated nuclear antigen I of Kaposi sarcoma Herpes virus. Molecular Immunology *44*, 1352–1360.